Two Decades of Array Signal Processing Research

The Parametric Approach

HAMID KRIM and MATS VIBERG

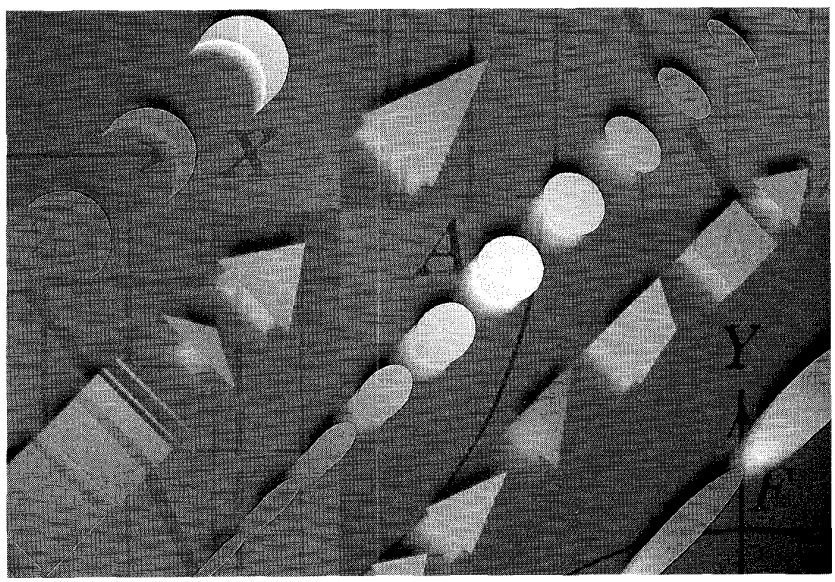

Estimation problems in theoretical as well as applied statistics have long been of great research interest given their importance in a great variety of applications. Parameter estimation has particularly been an area of focus by applied statisticians and engineers as problems required ever improving performance [7, 8, 9]. Many techniques were the result of an attempt by researchers to go beyond the classical Fourier-limit.

As applications expanded, the interest in accurately estimating relevant temporal as well as spatial parameters grew. Sensor array signal processing emerged as an active area of research and was centered on the ability to *fuse* data collected at several sensors in order to carry out a given estimation task (space-time processing). This framework, as will be described in more detail below, uses to advantage prior information on the data acquisition system (i.e., array geometry, sensor characteristics, etc.). The methods have proven useful for solving several real-world problems, perhaps most notably source localization in radar and sonar. Other more recent applications are discussed in later sections.

The first approach to carrying out space-time processing of data sampled at an array of sensors was spatial filtering or beamforming. The conventional (Bartlett) beamformer dates back to the second world-war, and is a mere application of Fourier-based spectral analysis to spatio-temporally sampled data. Later, adaptive beamformers [6, 25, 45] and classical time delay estimation techniques [8] were applied to enhance one's ability to resolve closely spaced signal sources. The spatial filtering approach, however, suffers from fundamental limitations: its performance, in particular, is directly dependent upon the physical size of the array (the aperture), regardless of the available data collection time and signal-to-noise ratio (SNR). From a statistical point of view, the classical techniques can be seen as spatial extensions of spectral Wiener filtering [150] (or *matched filtering*).

The extension of the time-delay estimation methods to more than one signal (these techniques originally used only two sensors), and the limited resolution of beamforming together with an increasing number of novel applications, renewed interest of researchers in statistical signal processing. We might add at this stage, that the word *resolution* is used in a rather informal way. It generally refers to the ability to distinguish closely spaced signal sources. One typically refers to some spectral-like measure, which would exhibit

1053-5888/96/$5.00©1996IEEE

peaks at the locations of the sources. Whenever there are two peaks near two actual emitters, the latter are said to be resolved. However, for parametric techniques, the intuitive notion of resolution is non-trivial to define in precise terms. This in turn, resulted in the emergence of the parameter estimation approach as an active research area. Important inspirations for the subsequent effort include the *Maximum Entropy* (ME) spectral estimation method in geophysics by [23] and early applications of the maximum likelihood principle [81, 106]. The introduction of subspace-based estimation techniques [13, 105] marked the beginning of a new era in the sensor array signal processing literature. The subspace-based approach relies on certain geometrical properties of the assumed data model, resulting in a resolution capability which (in theory) is not limited by the array aperture, provided the data collection time and/or SNR are sufficiently large and assuming the data model accurately reflects the experimental scenario.

The quintessential goal of sensor array signal processing is the *estimation of parameters* by fusing temporal and spatial information, captured via sampling a wavefield with a set of judiciously placed antenna sensors. The wavefield is assumed to be generated by a finite number of emitters, and contains information about signal parameters characterizing the emitters. Given the great number of existing applications for which the above problem formulation is relevant, and the number of newly emerging ones, we feel that a review of the area, with the hindsight and perspective provided by time, is in order. The focus is on parameter estimation methods, and many relevant problems are only briefly mentioned. The manuscript is clearly not meant to be exhaustive, but rather as a broad review of the area, and more importantly as a guide for a first time exposure to an interested reader. We deliberately emphasize the relatively more recent subspace-based methods in relation to *beamforming*, for which the reader is referred for more in depth treatment to the excellent, and in some sense complementary, review by Van Veen and Buckley [133]. For more extended presentations, the reader is referred to textbooks such as [50, 52, 58, 102].

The balance of this article consists of the background material and of the basic problem formulation. Then we introduce spectral-based algorithmic solutions to the signal parameter estimation problem. We contrast these suboptimal solutions to parametric methods. Techniques derived from maximum likelihood principles as well as geometric arguments are covered. Later, a number of more specialized research topics are briefly reviewed. Then, we look at a number of real-world problems for which sensor array processing methods have been applied. We also include an example with real experimental data involving closely spaced emitters and highly correlated signals, as well as a manufacturing application example.

A student/practitioner who is somewhat familiar with the field might read the various sections sequentially. For a first-time exposure, however, it may be best to scan the applications section before the description and somewhat more mathematical treatment of the algorithms are discussed.

Background and Formulation

In this section, we motivate the data model assumed throughout this paper, via its derivation from first principles in physics. Statistical assumptions about data collection are stated and basic geometrical properties of the model are reviewed.

Wave Propagation

Many physical phenomena are either a result of waves propagating through a medium (displacement of molecules) or exhibit a wave-like physical manifestation. A wave propagation which may take various forms (with variations depending on the phenomenon and on the medium, e.g. an electro-magnetic (EM) wave in free space or an acoustic wave in a pipe), generally follows from the homogeneous solution of the wave equation.

The models of interest in this paper may equally apply to an EM wave as well as to an acoustic wave (e.g., SONAR). Given that the propagation model is fundamentally the same, we will for analytical expediency, show that it can follow from the solution of Maxwell's equations, which, clearly are only valid for EM waves. In empty space (no current or charge) the following holds

$$\nabla \cdot \mathbf{E} = 0 \tag{1}$$

$$\nabla \cdot \mathbf{B} = 0 \tag{2}$$

$$\nabla \times \mathbf{E} = -\frac{\partial \mathbf{B}}{\partial t} \tag{3}$$

$$\nabla \times \mathbf{B} = \varepsilon_0 \mu_0 \frac{\partial \mathbf{E}}{\partial t} \tag{4}$$

where $\cdot$, and $\times$, respectively, denote the "divergence" and "curl." Further, $\mathbf{B}$ is the magnetic induction, $\mathbf{E}$ is the electric field, whereas μ_0 and ε_0 are the magnetic and dielectric constants. Invoking Eq. 1 the following curl property results,

$$\nabla \times (\nabla \times \mathbf{E}) = \nabla(\nabla \cdot \mathbf{E}) - \nabla^2 \mathbf{E} = -\nabla^2 \mathbf{E} . \tag{5}$$

Using Eqs. 3 and 4 leads to

$$\nabla \times (\nabla \times \mathbf{E}) = -\frac{\partial}{\partial t}(\nabla \times \mathbf{B}) = -\varepsilon_0 \mu_0 \frac{\partial^2 \mathbf{E}}{\partial t^2} , \tag{6}$$

which, when combined with Eq. 5, yields the fundamental wave equation

$$\nabla^2 \mathbf{E} - \frac{1}{c^2} \frac{\partial^2}{\partial t^2} \mathbf{E} = 0 . \tag{7}$$

The constant c is generally referred to as the speed of propagation, and for EM-waves in free space it follows from the above derivation $c = 1/\sqrt{\varepsilon_0 \mu_0} \approx 3 \times 10^8 \text{ m/s}$. The *homogeneous* (no forcing function) wave equation (Eq. 7) constitutes the physical motivation for our assumed data model. This is regardless of the type of wave or medium (EM or acoustic). In some applications, the underlying physics are irrelevant, it is merely the mathematical structure of the data model that counts.

Though Eq. 7 is a vector equation, we only consider one of its components, say $E(\mathbf{r},t)$ where $\mathbf{r}$ is the radius vector. It will later be assumed that the measured sensor outputs are proportional to $E(\mathbf{r},t)$. Interestingly enough, any field of the form $E(\mathbf{r},t) = f(t-\mathbf{r}^T\alpha)$ satisfies Eq. 7, , provided $|\alpha| = 1/c$, with "T" denoting transposition. Through its dependence on $t-\mathbf{r}^T\alpha$ only, the solution can be interpreted as a wave traveling in the direction α, with the speed of propagation $1/|\alpha| = c$. For the latter reason, α is referred to as the slowness vector. The chief interest herein is in narrowband (This is not really a restriction, since any signal can be expressed as a linear combination of narrowband components.) forcing functions. The details of generating such a forcing function (i.e. radiation of an antenna) can be found in the classic book by Jordan [59]. In complex notation (see e.g. [63, Section 15.3]) and taking the origin as a reference, a narrowband transmitted waveform can be expressed as (uppercase and lowercase Greek letters are to be understood as vectors or matrices within their context)

$$E(0,t) = s(t)e^{j}\omega^{t},$$

where $s(t)$ is slowly time-varying compared to the carrier $e^{j}\omega^{t}$. For $|\mathbf{r}| << c/B$, where B is the bandwidth of $s(t)$, we can write

$$E(\mathbf{r},t) = s\left(t-\mathbf{r}^{T}\alpha\right)e^{j\omega\left(t-\mathbf{r}^{T}\alpha\right)} \equiv s(t)e^{j\left(\omega t-\mathbf{r}^{T}\mathbf{k}\right)} \tag{8}$$

In the last equality the so-called wave-vector $\mathbf{k} = \alpha\omega$ was introduced, and its magnitude $|\mathbf{k}| = k = \omega/c$ is the wavenumber. One can also write $k = 2\pi/\lambda$, where λ is the wavelength. Note that $\mathbf{k}$ also points in the direction of propagation. For example, in the xy-plane we have

$$\mathbf{k} = k\left(\cos\theta \;\; \sin\theta\right)^{T}, \tag{9}$$

where θ is the direction of propagation, defined counterclockwise relative the x-axis (Fig. 1).

It should be noted that Eq. 8 implicitly assumed far-field conditions, since an isotropic (Isotropic refers to uniform propagation/transmission in all directions.) point source gives rise to a spherical traveling wave whose amplitude is inversely proportional to the distance to the source. All points lying on the surface of a sphere of radius R will then share a common phase and are referred to as a *wavefront*. This indicates that the distance between the emitters and the receiving antenna array determines whether the sphericity of the wave should be taken into account. The reader is referred to e.g., [10, 24] for treatments of near field reception. Far-field receiving conditions imply that the radius of propagation is so large (compared to the physical size of the array) that a flat plane of constant phase can be considered, thus resulting in a *plane wave* as indicated in Eq. 8. Though not necessary, the latter will be our assumed working model for convenience of exposition.

Note that a linear medium implies the validity of the superposition principle, and thus allows for more than one traveling wave. Equation 8 carries both spatial and temporal information and represents an adequate model for distinguishing signals with distinct spatio-temporal parameters. These may come in various forms, such as DOA (in general azimuth and elevation), signal polarization (if more than one component of the wave is taken into account), transmitted waveforms, temporal frequency etc. Each emitter is generally associated with a set of such characteristics. The interest in unfolding the signal parameters forms the essence of sensor array signal processing as presented herein, and continues to be an important and active topic of research.

Parametric Data Model

Most modern approaches to signal processing are model-based, in the sense that they rely on certain assumptions made on the observed data. In this section we describe the prevailing model used in the remainder of this article. A sensor is represented as a point receiver at given spatial coordinates. In the 2D-case and as shown in Fig. 1, we have $\mathbf{r}_l = (x_l \; y_l)^T$. Using Eqs, 8 and 9, the field measured at sensor l and due to a source at azimuthal DOA θ is given by

$$E(\mathbf{r}_l,t) = s(t)e^{\left[j\omega t-k\left(x_l\cos\theta+y_l\sin\theta\right)\right]}. \tag{10}$$

If a flat frequency response, say $g_l(\theta)$, is assumed for the sensor l over the signal bandwidth, its measured output will be proportional to the field at $\mathbf{r}_l$. Dropping the carrier term $e^{j}\omega^{t}$ for convenience (in practice, the signal is usually down-converted to baseband before sampling), the output is modeled by

$$x_l(t) = g_l(\theta)e^{-jk\left(x_l\cos\theta+y_l\sin\theta\right)}s(t) = a_l(\theta)s(t) \tag{11}$$

Referring to Eq. 8, we see that Eq. 11 requires that the array aperture (i.e. the physical size measured in wavelengths) be much less than the inverse relative bandwidth

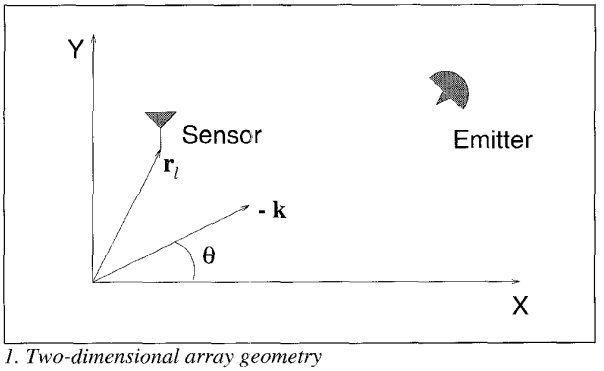

1. Two-dimensional array geometry

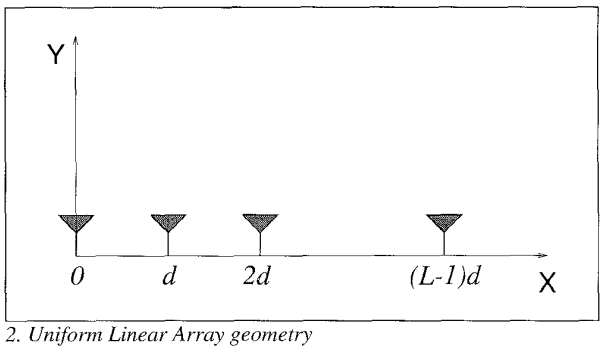

2. Uniform Linear Array geometry

(*f*/*B*). In the array processing literature, this is referred to as the *narrowband assumption*. For an L-element antenna array of arbitrary geometry, the array output vector is obtained as

$$\mathbf{x}(t) = \mathbf{a}(\theta)s(t).$$

A single signal at the DOA θ, thus results in a scalar multiple of the *steering vector* (Other popular names for $\mathbf{a}(\theta)$ include action vector, array propagation vector and signal replica vector.) $\mathbf{a}(\theta) = [a_1(\theta),...,a_L(\theta)]^T$ as the array output. Common array geometries are depicted in Figs. 2 and 3. For the uniform linear array (ULA) we have $\mathbf{r}_l = ((l-1)d\ \ 0)^T$, and assuming that all elements have the same directivity $g_1(\theta) = \ldots = g_L(\theta) = g(\theta)$, the ULA steering vector takes the form (cf. (11))

$$\mathbf{a}_{\mathrm{ULA}}(\theta) = g(\theta)\left[1 \quad e^{-jkd\cos\theta} \quad \cdots \quad e^{-j(L-1)kd\cos\theta}\right]^T, \tag{12}$$

where d denotes the inter-element distance. The radius vectors of the uniform circular array (UCA) have the form $\mathbf{r}_l = R(\cos(2\pi(l-1)/L)\ \sin(2\pi(l-1)/L))^T$, from which the form of the UCA steering vector can easily be derived. As previously alluded to, a signal source can be associated with a number of characteristic parameters. For the sake of clarity and ease of presentation by referring to Figs. 2 and 3, we assume that θ is a real-valued scalar referred to as the DOA. For most of the discussed methods the extension to the multiple parameter per source case is straightforward.

As noted earlier, the superposition principle is applicable assuming a linear receiving system. If M signals impinge on an L-dimensional array from distinct DOAs $\theta_1,...,\theta_M$, the output vector takes the form

$$\mathbf{x}(t) = \sum_{m=1}^{M} \mathbf{a}(\theta_m)s_m(t),$$

where $s_m(t)$, $m = 1,..., M$ denote the baseband signal waveforms. The output equation can be put in a more compact form by defining a steering matrix and a vector of signal waveforms as

$$\mathbf{A}(\theta) = \left[\mathbf{a}(\theta_1),\ldots,\mathbf{a}(\theta_M)\right] \quad (L \times M)$$
$$\mathbf{s}(t) = \left[s_1(t),\ldots,s_M(t)\right]^T$$

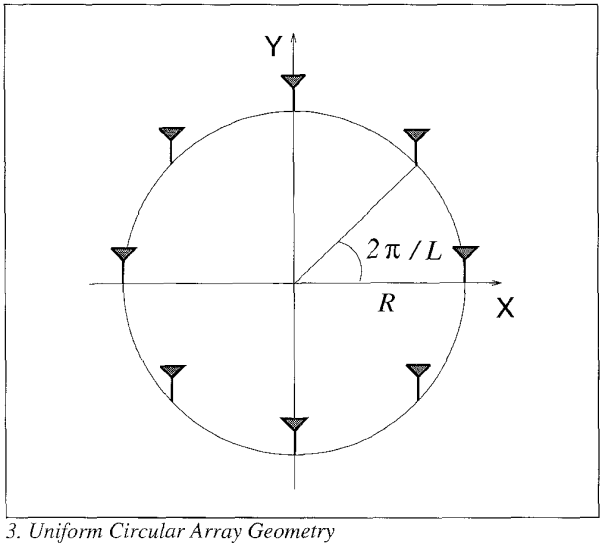

3. Uniform Circular Array Geometry

In the presence of an additive noise $\mathbf{n}(t)$ we now get the model commonly used in array processing

$$\mathbf{x}(t) = \mathbf{A}(\theta)\mathbf{s}(t) + \mathbf{n}(t). \tag{13}$$

The methods to be presented all require that $M < L$, which is therefore assumed throughout the development. It is interesting to note that in the noiseless case, the array output is then confined to an M-dimensional subspace of the complex L-space, which is spanned by the steering vectors. This is the signal subspace, and this observation forms the basis of subspace-based methods .

The sensor outputs are appropriately pre-processed and sampled at arbitrary time instances, labeled $t = 1,2,...,N$ for simplicity. Clearly, the process $\mathbf{x}(t)$ can be viewed as a multichannel random process, whose characteristics can be well understood from its first and second order statistics determined by the underlying signals and noise. The preprocessing of the signal is often done in such a way that $\mathbf{x}(t)$ can be regarded as temporally white.

Assumptions

The signal parameters which are of interest in this article are spatial in nature, and thus require the cross-covariance information among the various sensors, i.e. the *spatial covariance matrix*

$$\mathbf{R} = \mathrm{E}\{\mathbf{x}(t)\mathbf{x}^H(t)\} = \mathbf{A}\mathrm{E}\{\mathbf{s}(t)\mathbf{s}^H(t)\}\mathbf{A}^H + \mathrm{E}\{\mathbf{n}(t)\mathbf{n}^H(t)\} \tag{14}$$

where $\mathrm{E}\{\cdot\}$ denotes statistical expectation,

$$\mathrm{E}\{\mathbf{s}(t)\mathbf{s}^H(t)\} = \mathbf{P} \tag{15}$$

is the source covariance matrix and

$$\mathbf{E}\left\{\mathbf{n}(t)\mathbf{n}^H(t)\right\} = \sigma^2\mathbf{I} \tag{16}$$

is the noise covariance matrix. The latter covariance structure is a reflection of the noise having a common variance σ^2 at all sensors and being uncorrelated among all sensors. Such noise is usually termed *spatially white*, and is a reasonable model, for example receiver noise. However, other man-made noise sources need not result in spatial whiteness, in which case the noise must be pre-whitened in many of the methods to be described. More specifically, if the noise covariance matrix is $\mathbf{Q}$, the sensor outputs are multiplied by $\mathbf{Q}^{-1/2}$ ($\mathbf{Q}^{-1/2}$ denotes a Hermitian square-root factor of $\mathbf{Q}^{-1}$) prior to further processing. The source covariance matrix, $\mathbf{P}$, is often assumed to be nonsingular (a rank-deficient $\mathbf{P}$, as in the case of coherent signals, is discussed later) or near-singular for highly correlated signals.

In the later development, the spectral factorization of $\mathbf{R}$ will be of central importance, and its positivity guarantees the following representation,

$$\mathbf{R} = \mathbf{A}\mathbf{P}\mathbf{A}^H + \sigma^2\mathbf{I} = \mathbf{U}\Lambda\mathbf{U}^H, \tag{17}$$

with $\mathbf{U}$ unitary and $\Lambda = \text{diag}\{\lambda_1, \lambda_2, \ldots, \lambda_L\}$ a diagonal matrix of real eigenvalues ordered such that $\lambda_1 \geq \lambda_2 \geq \ldots \geq \lambda_L > 0$. Observe that any vector orthogonal to $\mathbf{A}$ is an eigenvector of $\mathbf{R}$ with the eigenvalue σ^2. There are $L - M$ linearly independent such vectors. Since the remaining eigenvalues are all larger than σ^2, we can partition the eigenvalue/vector pairs into noise eigenvectors (corresponding to eigenvalues $\lambda_{M+1} = \ldots = \geq \lambda_L = \sigma^2$) and signal eigenvectors (corresponding to eigenvalues $\lambda_1 \geq \ldots \geq \lambda_M > \sigma^2$). Hence, we can write

$$\mathbf{R} = \mathbf{U}_s\Lambda_s\mathbf{U}_s^H + \mathbf{U}_n\Lambda_n\mathbf{U}_n^H, \tag{18}$$

where $\Lambda_n = \sigma^2\mathbf{I}$. Since all noise eigenvectors are orthogonal to $\mathbf{A}$, the columns of $\mathbf{U}_s$ must span the range space of $\mathbf{A}$ whereas those of $\mathbf{U}_n$ span its orthogonal complement (the nullspace of $\mathbf{A}^H$). The projection operators onto these signal and noise subspaces are defined as

$$\begin{aligned} \Pi &= \mathbf{U}_s\mathbf{U}_s^H = \mathbf{A}\left(\mathbf{A}^H\mathbf{A}\right)^{-1}\mathbf{A}^H \\ \Pi^{\perp} &= \mathbf{U}_n\mathbf{U}_n^H = \mathbf{I} - \mathbf{A}\left(\mathbf{A}^H\mathbf{A}\right)^{-1}\mathbf{A}^H, \end{aligned} \tag{19}$$

provided that the inverse in the expressions exists. It then follows

$$\mathbf{I} = \Pi + \Pi^{\perp} \tag{20}$$

Problem Definition

The problem of central interest herein is that of estimating the DOAs of emitter signals impinging on a receiving array, when given a finite data set $\{\mathbf{x}(t)\}$ observed over $t = 1,2,\ldots,N$. As noted earlier, we will primarily focus on reviewing a number of techniques based on second-order statistics of data.

All of the earlier formulation assumed the existence of exact quantities, i.e. infinite observation time. It is clear that in practice only sample estimates which we denote by a hat, i.e., $\hat{}$, are available. A natural estimate of $\mathbf{R}$ is the sample covariance matrix

$$\hat{\mathbf{R}} = \frac{1}{N}\sum_{t=1}^{N}\mathbf{x}(t)\mathbf{x}^H(t), \tag{21}$$

for which a spectral representation similar to that of $\mathbf{R}$ is defined as

$$\hat{\mathbf{R}} = \hat{\mathbf{U}}_s\hat{\Lambda}_s\hat{\mathbf{U}}_s^H + \hat{\mathbf{U}}_n\hat{\Lambda}_n\hat{\mathbf{U}}_n^H. \tag{22}$$

This representation will be extensively used in the description and implementation of the subspace-based estimation algorithms. Indeed, if $\mathbf{x}(t)$ is a stationary white Gaussian process with unknown structure (i.e., the data model (13) is not used), then $\hat{\mathbf{R}}$ and its eigen-elements are maximum likelihood estimates of the corresponding exact quantities [4].

Throughout the paper, the number of underlying signals, M, in the observed process is considered known. There are, however, good and consistent techniques for estimating the M signals present [31, 68, 108, 144] in the event that such information is not available (see also the "Additional Topics"). In the following two sections we discuss the best known parameter estimation techniques, respectively classified as *Spectral-Based* and *Parametric* methods. Due to space limitations, a number of good variations which address specific aspects of the underlying problem and which have appeared in the literature are overlooked. Our reference list attempts to cover a portion of the gap which clearly can never be filled.

Summary of Estimators

Since the number of algorithms is extensive, it makes sense to give an overview of their properties already at this stage. The following "glossary" is useful for this purpose:

- *Coherent signals* Two signals are coherent if one is a scaled and delayed version of the other.
- *Consistency* An estimate is consistent if it converges to the true value when the number of data tends to infinity.
- *Statistical efficiency* An estimator is statistically efficient if it asymptotically attains the Cramér-Rao Bound (CRB), which is a lower bound on the covariance matrix of any unbiased estimator (see e.g. [63]).

We will distinguish between methods that are applicable to arbitrary array geometries and those that require a uniform linear array. Tables 1 and 2 summarize the message conveyed in the algorithm descriptions. The major computational requirements for each method are also included, assuming that the sample covariance matrix has already been acquired. Here, 1-D search means that the parameter estimates are computed from M one-dimensional searches over the parameter space, whereas M-D search refers to a full M-dimen-

Table 1: Summary of Estimators Applicable to Arbitrary Array Geometries				
Method	Consistency	Coherent Signals	Statistical Performance	Computations
Bartlett	$M = 1$	-	-	1-D Search
Capon	No	No	Poor	1-D Search
MUSIC	Yes	No	Good	EVD, 1-D Search
Min-Norm	Yes	No	Good	EVD, 1-D Search
DML	Yes	Yes	Good	M-D Search
SML	Yes	Yes	Efficient	M-D Search
WSF	Yes	Yes	Efficient	EVD, M-D Search

Table 2: Summary of Estimators Applicable to Uniform Linear Arrays				
Method	Consistency	Coherent Signals	Statistical Performance	Computations
Root-Music	Yes	Yes	Good	EVD, polynomial
ESPRIT	Yes	Yes	Good	EVD
IQML	Yes	Yes	Good	Iterative
Root-WSF	Yes	Yes	Efficient	EVD, LS

sional numerical optimization. By a "good" statistical performance, we mean that the theoretical mean square error of the estimates is close to the CRB, typically within a few dB in practical scenarios.

Spectral-Based Algorithmic Solutions

As mentioned earlier, we classify the parameter estimation techniques into two main categories, namely *spectral-based* and *parametric* approaches. In the former, one forms some spectrum-like function of the parameter(s) of interest, e.g., the DOA. The locations of the highest (separated) peaks of the function in question are recorded as the DOA estimates. Parametric techniques, on the other hand, require a simultaneous search for all parameters of interest. The latter approach often results in more accurate estimates, albeit at the expense of an increased computational complexity.

Spectral-based methods which are discussed in this section, can be classified into beamforming techniques and subspace-based methods.

Beamforming Techniques

The first attempt to automatically localize signal sources using antenna arrays was through beamforming techniques. The idea is to "steer" the array in one direction at a time and measure the output power. The steering locations which result in maximum power yield the DOA estimates. The array response is steered by forming a linear combination of the sensor outputs

$$y(t) = \sum_{i=1}^{L} w_i^* x_i(t) = \mathbf{w}^H \mathbf{x}(t). \tag{23}$$

Given samples $y(1), y(2), \ldots, y(N)$, the output power is measured by

$$P(\mathbf{w}) = \frac{1}{N}\sum_{t=1}^{N} |y(t)|^2 = \frac{1}{N}\sum_{t=1}^{N} \mathbf{w}^H \mathbf{x}(t)\mathbf{x}^H(t)\mathbf{w} = \mathbf{w}^H \hat{\mathbf{R}} \mathbf{w} \tag{24}$$

where $\hat{\mathbf{R}}$ is defined in (21). Different beamforming approaches correspond to different choices of the weighting vector $\mathbf{w}$. For an excellent review of beamforming methods, we refer to [132].

Conventional Beamformer

The conventional (or Bartlett) beamformer is a natural extension of classical Fourier-based spectral analysis [12] to sensor array data. For an array of arbitrary geometry, this algorithm maximizes the power of the beamforming output for a given input signal. Suppose we wish to maximize the output power from a certain direction θ. Given a signal emanating from direction θ, a measurement of the array output is corrupted by additive noise and written as

$$\mathbf{x}(t) = \mathbf{a}(\theta)s(t) + \mathbf{n}(t).$$

The problem of maximizing the output power is then formulated as,

$$\max_{\mathbf{w}} \mathrm{E}\{\mathbf{w}^H\mathbf{x}(t)\mathbf{x}^H(t)\mathbf{w}\} = \max_{\mathbf{w}} \mathbf{w}^H\mathrm{E}\{\mathbf{x}(t)\mathbf{x}^H(t)\}\mathbf{w} \qquad (25)$$
$$= \max_{\mathbf{w}}\{\mathrm{E}|s(t)|^2|\mathbf{w}^H\mathbf{a}(\theta)|^2 + \sigma^2|\mathbf{w}|^2\},$$

where the assumption of spatially white noise is used. To obtain a non-trivial solution, the norm of $\mathbf{w}$ is constrained to $|\mathbf{w}| = 1$ when carrying out the above maximization. The resulting solution is then

$$\mathbf{w}_{BF} = \frac{\mathbf{a}(\theta)}{\sqrt{\mathbf{a}^H(\theta)\mathbf{a}(\theta)}} \qquad (26)$$

The above weight vector can be interpreted as a spatial filter, which has been matched to the impinging signal. Intuitively, the array weighting equalizes the delays (and possibly attenuations) experienced by the signal on various sensors to maximally combine their respective contributions.

Inserting the weighting vector Eq. 26 into Eq. 24, the classical *spatial spectrum* is obtained

$$P_{BF}(\theta) = \frac{\mathbf{a}^H(\theta)\hat{\mathbf{R}}\mathbf{a}(\theta)}{\mathbf{a}^H(\theta)\mathbf{a}(\theta)}. \qquad (27)$$

For a uniform linear array of isotropic sensors, the steering vector $\mathbf{a}(\theta)$ takes the form (cf. (12))

$$\mathbf{a}_{\mathrm{ULA}}(\theta) = \begin{bmatrix} 1 & e^{j\phi} & \cdots & e^{j(L-1)\phi} \end{bmatrix}^T, \qquad (28)$$

where

$$\phi = -kd\cos\theta = -\frac{\omega}{c}d\cos\theta \qquad (29)$$

is termed the *electrical angle*. By inserting Eq. 28 into Eq. 27, and noting that $|\mathbf{a}_{ULA}(\theta)|^2 = M$, we obtain $P_{BF}(\theta)$ as the spatial analogue of the classical periodogram in temporal time series analysis, see e.g. [96]. Unfortunately, the spatial spectrum shares the same resolution limitation as the periodogram. The standard beamwidth for a ULA is $\phi_B = 2\pi/L$, and sources whose electrical angles are closer than ϕ_B will not be resolved by the conventional beamformer, regardless of the available data quality. This point is illustrated in Figure 4, where the beamforming spectrum is plotted versus the DOA in two different scenarios. A ULA of $M = 10$ sensors of half-wavelength inter-element spacing (Such a ULA is often termed a standard ULA, because $d = \pi/k$ is the maximum allowable element separation to avoid ambiguities.) is used to separate two uncorrelated emitters, based on a batch of $N = 100$ data samples. The signal-to-noise ratio (SNR) for both sources is 0 dB. The beamwidth for such an array is $2\pi/10 \approx 0.63$, implying that sources need to be at least 12° apart in order to be separated by the beamformer. This is also verified in the figure, because for 10° separation, the sources are nearly (but not quite) resolved.

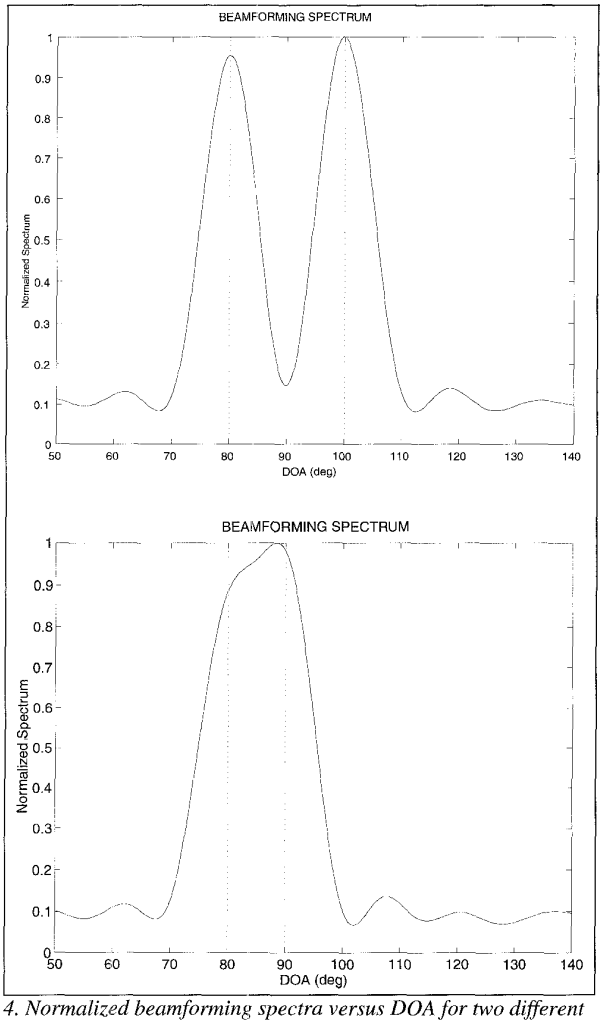

4. Normalized beamforming spectra versus DOA for two different scenarios. True DOAs indicated by dotted vertical lines

Capon's Beamformer

In an attempt to alleviate the limitations of the above beamformer, such as its resolving power of two sources spaced closer than a beamwidth, researchers have proposed numerous modifications. A well-known method was proposed by Capon [25], and was later interpreted as a dual of the beamformer by Lacoss [74]. The optimization problem was posed as

$$\min_{\mathbf{w}} P(\mathbf{w}) \quad \text{subject to } \mathbf{w}^H\mathbf{a}(\theta) = 1, \qquad (30)$$

where $P(\mathbf{w})$ is as defined in Eq. 24. Hence, Capon's beamformer (also known as the Minimum Variance Distorsionless Response filter in the acoustics literature) attempts to minimize the power contributed by noise and any signals coming from other directions than θ, while maintaining a fixed gain in the "look direction" θ. (This can be viewed as a sharp spatial bandpass filter.) The optimal $\mathbf{w}$ can be found using, e.g., the technique of Lagrange multipliers, resulting in

$$\mathbf{w}_{CAP} = \frac{\hat{\mathbf{R}}^{-1}\mathbf{a}(\theta)}{\mathbf{a}^H(\theta)\hat{\mathbf{R}}^{-1}\mathbf{a}(\theta)}. \quad (31)$$

Inserting the above weight into (24) leads to the following "spatial spectrum"

$$P_{CAP}(\theta) = \frac{1}{\mathbf{a}^H(\theta)\hat{\mathbf{R}}^{-1}\mathbf{a}(\theta)}. \quad (32)$$

It is easy to see why Capon's beamformer outperforms the classical one given in Eq. 27, as the former uses every available degree of freedom to concentrate the received energy along one direction, namely the bearing of interest. This is reflected by the constraint given in Eq. 30. The power minimization can also be interpreted as sacrificing some noise suppression capability for more focused "nulling" in the directions where there are other sources present. The spectral leakage from closely spaced sources is therefore reduced, though the resolution capability of the Capon beamformer is still dependent upon the array aperture and clearly on the SNR. A number of alternative methods for beamforming have been proposed, addressing various issues such as partial signal cancelling due to signal coherence [149] and beam shaping and interference control [22, 44, 132].

Subspace-Based Methods

Many spectral methods in the past, have implicitly called upon the spectral decomposition of a covariance matrix to carry out the analysis (e.g., Karhunen-Loève representation). One of the most significant contributions came about when the eigen-structure of the covariance matrix was explicitly invoked, and its intrinsic properties were directly used to provide a solution to an underlying estimation problem for a given observed process. Early approaches involving invariant subspaces of observed covariance matrices include principal component factor analysis [55] and errors-in-variables time series analysis [65]. In the engineering literature, Pisarenko's work [94] in harmonic retrieval was among the first to be published. However, the tremendous interest in the subspace approach is mainly due to the introduction of the MUSIC (Multiple SIgnal Classification) algorithm [13, 105]. It is interesting to note that while earlier works were mostly derived in the context of time series analysis and later applied to the sensor array problem, MUSIC was indeed originally presented as a DOA estimator. It has later been successfully brought back to the spectral analysis/system identification problem with its later developments (see e.g. [118, 135]).

The MUSIC Algorithm

As noted previously, the structure of the exact covariance matrix with the spatial white noise assumption implies that its spectral decomposition can be expressed as

$$\mathbf{R} = \mathbf{A}\mathbf{P}\mathbf{A}^H + \sigma^2\mathbf{I} = \mathbf{U}_s\Lambda_s\mathbf{U}_s^H + \sigma^2\mathbf{U}_n\mathbf{U}_n^H, \quad (33)$$

where, assuming $\mathbf{APA}^H$ to be of full rank, the diagonal matrix Λ_S contains the M largest eigenvalues. Since the eigenvectors in $\mathbf{U}_n$ (the noise eigenvectors) are orthogonal to $\mathbf{A}$, we have

$$\mathbf{U}_n^H\mathbf{a}(\theta) = 0, \quad \theta \in \{\theta_1,\ldots,\theta_M\} \quad (34)$$

To allow for unique DOA estimates, the array is usually assumed to be *unambiguous*; that is, any collection of L steering vectors corresponding to distinct DOAs η_k forms a linearly independent set $\{a(\eta_1),\ldots,a(\eta_L)\}$ (recall $M < L$). If $\mathbf{a}(\cdot)$ satisfies these conditions and $\mathbf{P}$ has full rank, then $\mathbf{APA}^H$ is also of full rank. It then follows that $\theta_1,\ldots,\theta_M$ are the only possible solutions to the relation in Eq. 34, which could therefore be used to exactly locate the DOAs.

In practice, an estimate $\hat{\mathbf{R}}$ of the covariance matrix is obtained, and its eigenvectors are separated into the signal and noise eigenvectors as in Eq. 22. The orthogonal projector onto the noise subspace is estimated as

$$\hat{\Pi}^{\perp} = \hat{\mathbf{U}}_n\hat{\mathbf{U}}_n^H. \quad (35)$$

The MUSIC "spatial spectrum" is then defined as

$$P_M(\theta) = \frac{\mathbf{a}^H(\theta)\mathbf{a}(\theta)}{\mathbf{a}^H(\theta)\hat{\Pi}^{\perp}\mathbf{a}(\theta)}. \quad (36)$$

Although $P_M(\theta)$ is not a true spectrum in any sense (it is merely the distance between two subspaces), it exhibits peaks in the vicinity of the true DOAs, as suggested by (34). The performance of the various spectral-based estimators is illustrated in Fig. 5, where the scenario is identical to that of Fig. 4.

The performance improvement of the MUSIC estimator was so significant that it became an alternative to most existing methods. In particular, it follows from the above reasoning that estimates of an arbitrary accuracy can be

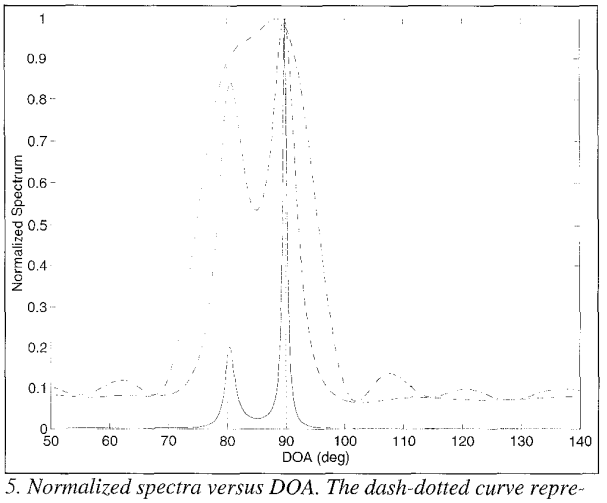

5. Normalized spectra versus DOA. The dash-dotted curve represents the conventional beamformer, the dashed curve is Capon's method and the solid curve is the "Music Spectrum." True DOAs indicated by dotted vertical lines.

obtained if the data collection time is sufficiently long or the SNR is adequately high, and the signal model is sufficiently accurate. Thus, in contrast to the beamforming techniques, the MUSIC algorithm provides *statistically consistent* estimates. Though the MUSIC functional (Eq. 36) does not represent a spectral estimate, its important limitation is still the failure to resolve closely spaced signals in small samples and at low SNR scenarios. This loss of resolution is more pronounced for highly correlated signals. In the limiting case of coherent signals, the property (Eq. 34) is violated and the method fails to yield consistent estimates, see e.g. [67]. The mitigation of this limitation is an important issue and is separately addressed at the end of this section.

Extensions to MUSIC

The MUSIC algorithm spawned a significant increase in research activity which led to a multitude of proposed modifications. These were attempts to improve/overcome some of its shortcomings in various specific scenarios. The most notable was the unifying theme of *weighted MUSIC* which, for different $\mathbf{W}$, particularized to various algorithms

$$P_{WM}(\theta) = \frac{\mathbf{a}^H(\theta)\mathbf{a}(\theta)}{\mathbf{a}^H(\theta)\hat{\Pi}^{\perp}\mathbf{W}\hat{\Pi}^{\perp}\mathbf{a}(\theta)}. \tag{37}$$

The weighting matrix $\mathbf{W}$ is introduced to take into account (if desired) the influence of each of the eigenvectors. It is clear that a uniform weighting of the eigenvectors, i.e. $\mathbf{W} = \mathbf{I}$, results in the original MUSIC method. As shown in [114], this is indeed the optimal weighting in terms of yielding estimates of minimal asymptotic variance. However, in difficult scenarios involving small samples, low SNR and highly correlated signals, a carefully chosen non-uniform weighting may still improve the resolution capability of the estimator without seriously increasing the variance.

One particularly useful choice of weighting is given by [69]

$$\mathbf{W} = \mathbf{e}_1\mathbf{e}_1^T, \tag{38}$$

where $\mathbf{e}_1$ is the first column of the L x L identity matrix. This corresponds to the Min-Norm algorithm, derived in [72, 99] for ULAs and extended to arbitrary arrays in [75]. As shown in [61], the Min-Norm algorithm indeed exhibits a lower bias and hence a better resolution than the original MUSIC algorithm, at least when applied to ULAs.

Resolution-Enhanced Spectral Based Methods

The MUSIC algorithm is known to enjoy a property of high accuracy in estimating the phases of the roots corresponding to DOA of sources. The bias in the estimates' radii [69], however, affects the resolution of closely spaced sources when using the spatial spectrum.

A solution first proposed in [14], and later in [21, 40], is to couple the MUSIC algorithm with some spatial prefiltering, to result in what is known as *Beamspace Processing*. This is indeed equivalent to preprocessing the received data with a predefined matrix $\mathbf{T}$, whose columns can be chosen as the steering vectors for a set of chosen directions:

$$\mathbf{z}(t) = \mathbf{T}^H\mathbf{x}(t) \tag{39}$$

Clearly, the steering vectors $\mathbf{a}(\theta)$ are then replaced by $\mathbf{T}^H\mathbf{a}(\theta)$ and the noise covariance for the beamspace data becomes $\sigma^2\mathbf{T}^H\mathbf{T}$. For the latter reason, $\mathbf{T}$ is often made orthogonal and of norm 1 before application to $\mathbf{x}(t)$.

It is clear that if a certain spatial sector is selected to be swept (e.g. some prior knowledge about the broad direction of arrival of the sources may be available), one can potentially experience some gain, the most obvious being computational, as a smaller dimensionality of the problem usually results. It has, in addition, been shown that the bias of the estimates is decreased when employing MUSIC in beamspace as opposed to the "element space" MUSIC [40, 158]. As expected, the variance of the DOA estimates is not improved, but a certain robustness to spatially correlated noise has been noted in [40]. The latter fact can intuitively be understood when one recalls that the spatial pre-filter has a bandpass character, which will clearly tend to whiten the noise.

Other attempts to improving the resolution of the MUSIC method are presented in [35, 62, 156], based on different modifications of the criterion function.

Coherent Signals

Though unlikely that one would deliberately transmit two coherent signals from distinct directions, such a phenomenon is not uncommon as either a natural result of a multipath propagation effect, or intentional unfriendly jamming. The end result is a rank deficiency in the source covariance matrix $\mathbf{P}$. This, in turn, results in a divergence of a signal eigenvector into the noise subspace. Therefore, in general $\mathbf{U}_n^H\mathbf{a}(\theta) \neq 0$ for any θ and the MUSIC "spectrum" may fail to produce peaks at the DOA locations. In particular, the ability to resolve closely spaced sources is dramatically reduced for highly correlated signals, e.g., [70].

In the simple case of two coherent sources being present and a uniform linear array, there is a fairly straightforward way to "de-correlate" the signals. The idea is to employ a forward-backward (FB) averaging as follows. Note that a ULA steering vector (28) remains invariant, up to a scaling, if its elements are reversed and complex conjugated. More precisely, let $\mathbf{J}$ be an L L exchange matrix, whose components are zero except for ones on the anti-diagonal. Then, for a ULA it holds that

$$\mathbf{J}\mathbf{a}^*(\theta) = e^{-j(L-1)\phi}\mathbf{a}(\theta) \tag{40}$$

The so-called backward array covariance matrix therefore takes the form

$$\mathbf{R}_B = \mathbf{J}\mathbf{R}^*\mathbf{J} = \mathbf{A}\Phi^{-(L-1)}\mathbf{P}\Phi^{-(L-1)}\mathbf{A}^H + \sigma^2\mathbf{I}, \tag{41}$$

where Φ is a diagonal matrix with $e^{j\phi k}$, $k = 1,\ldots,M$ on the diagonal, and ϕ_k as previously defined. By averaging the usual array covariance and $\mathbf{R}_B$, one obtains the FB array covariance

$$\mathbf{R}_{FB} = \frac{1}{2}\left(\mathbf{R} + \mathbf{J}\mathbf{R}^*\mathbf{J}\right) = \mathbf{A}\tilde{\mathbf{P}}\mathbf{A}^H + \sigma^2\mathbf{I}, \tag{42}$$

where the new "source covariance matrix" $\tilde{\mathbf{P}} = \left(\mathbf{P} + \Phi^{-(L-1)}\mathbf{P}\Phi^{-(L-1)}\right)/2$ generally has full rank. The FB version of any covariance-based algorithm simply consists of replacing $\hat{\mathbf{R}}$ with $\hat{\mathbf{R}}_{FB}$, defined as in Eq. 42. Note that this transformation has also been used in noncoherent scenarios, and in particular in time series analysis, for merely improving the variance of the estimates.

In a more general scenario where more than two coherent sources are present, forward-backward averaging cannot restore the rank of the signal covariance matrix on its own. A heuristic solution of this problem was first proposed in [149] for uniform linear arrays, and later formalized and extended in [33, 43, 108]. The idea of the so-called *spatial smoothing* technique is to split the ULA into a number of overlapping subarrays, as illustrated in Figure 6. The steering vectors of the subarrays are assumed to be identical up to different scalings, and the subarray covariance matrices can therefore be averaged. Similar to (42), the spatial smoothing induces a random phase modulation which in turn tends to decorrelate the signals that caused the rank deficiency. A compact expression for this smoothed matrix $\tilde{\mathbf{R}}$ can be written in terms of selection matrices $\mathbf{F}_k$ as follows. Let p denote the number of elements in the subarrays, implying that the number of subarrays is $K = L - p + 1$. Then, the spatially smoothed array covariance matrix can be expressed as

$$\tilde{\mathbf{R}} = \frac{1}{K}\sum_{k=1}^{K}\mathbf{F}_k\mathbf{R}\mathbf{F}_k^T,$$
$$\text{with, } \mathbf{F}_k = \left[0_{P\times(k-1)}|\mathbf{I}_P|0_{P\times(L-k-P+1)}\right].$$

The rank of the averaged source covariance matrix $\tilde{\mathbf{R}}$ can be shown to increase by 1 with probability 1 [29] for each additional subarray in the averaging, until it reaches its maximum value M.

The drawback with spatial smoothing is that the effective aperture of the array is reduced, since the subarrays are smaller than the original array. However, despite this loss of aperture, the spatial smoothing transformation mitigates the limitation of all subspace-based estimation techniques while retaining the computational efficiency of the one-dimensional spectral searches. As discussed in the next section, the parametric techniques generally do not experience such problems when faced with coherent signals. They require, on the other hand, a more complicated multidimensional search. We again stress the fact that spatial smoothing is limited to regular arrays with a translational invariance property, and FB averaging requires a ULA. When using more general arrays (e.g. circular), some sort of transformation of the received data must precede the smoothing transformation. Such a transformation is conceptually possible, but generally requires some *a priori* knowledge of the source locations.

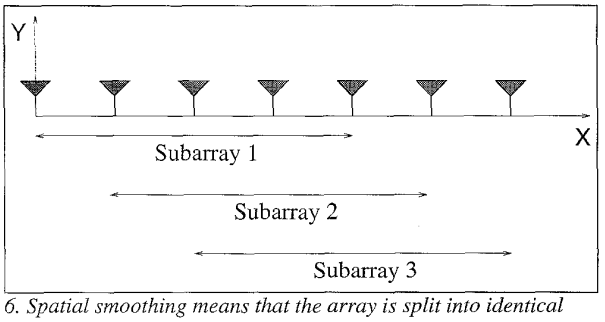

6. Spatial smoothing means that the array is split into identical subarrays, the covariances of which are averaged

Parametric Methods

While the spectral-based methods presented in the previous section are computationally attractive, they do not always yield sufficient accuracy. In particular, for scenarios involving highly correlated (or even coherent) signals, the performance of spectral-based methods may be insufficient. An alternative is to more fully exploit the underlying data model, leading to so-called *parametric* array processing methods. As we shall see, coherent signals impose no conceptual difficulties for such methods. The price to pay for this increased efficiency and robustness is that the algorithms typically require a multidimensional search to find the estimates. For uniform linear arrays (ULAs), the search can, however, be avoided with little (if any) loss of performance.

Perhaps the most well known and frequently used model-based approach in signal processing is the maximum likelihood (ML) technique. This methodology requires a statistical framework for the data generation process. Two different assumptions about the emitter signals have led to corresponding ML approaches in the array processing literature. In this section we will briefly review both of these approaches, discuss their relative merits, and present subspace-based ML approximations. Parametric DOA estimation methods are in general computationally quite complex. However, for ULAs a number of less demanding algorithms are known, as presented shortly.

Deterministic Maximum Likelihood

While the background and receiver noise in the assumed data model can be thought of as emanating from a large number of independent noise sources, the same is usually not the case for the emitter signals. It therefore appears natural to model the noise as a stationary Gaussian white random process whereas the signal waveforms are deterministic (arbitrary) and unknown. (The carrier frequencies are assumed to be known.) Assuming spatially white and circularly symmetric (A complex random process is circularly symmetric if its real

and imaginary parts are identically distributed and have a skew-symmetric cross-covariance, i.e., E[Re($\mathbf{n}(t)$)Im($\mathbf{n}^T(t)$)) = -E[Im($\mathbf{n}(t)$)Re($\mathbf{n}^T(t)$)]] noise, the second-order moments of the noise term take the form

$$\mathrm{E}\{\mathbf{n}(t)\mathbf{n}^H(s)\} = \sigma^2\mathbf{I}\delta_{t,s} \tag{43}$$

$$\mathrm{E}\{\mathbf{n}(t)\mathbf{n}^T(s)\} = 0. \tag{44}$$

As a consequence of the statistical assumptions, the observation vector $\mathbf{x}(t)$ is also a circularly symmetric and temporally white Gaussian random process, with mean $\mathbf{A}(\theta)\mathbf{s}(t)$ and covariance matrix $\sigma^2\mathbf{I}$. The *likelihood function* is the probability density function (PDF) of all observations given the unknown parameters. The PDF of one measurement vector $\mathbf{x}(t)$ is the complex L-variate Gaussian:

$$\frac{1}{(\pi\sigma^2)^L} e^{-\|\mathbf{x}(t)-\mathbf{A}\mathbf{s}(t)\|^2/\sigma^2}, \tag{45}$$

where $\|\cdot\|$ denotes the Euclidean norm, and the argument of $\mathbf{A}(\theta)$ has been dropped for notational convenience. Since the measurements are independent, the likelihood function is obtained as

$$L_{DML}(\theta, \mathbf{s}(t), \sigma^2) = \prod_{t=1}^{N} (\pi\sigma^2)^{-L} e^{-\|x(t)-\mathbf{A}\mathbf{s}(t)\|^2/\sigma^2} \tag{46}$$

As indicated above, the unknown parameters in the likelihood function are the signal parameters θ, the signal waveforms $\mathbf{s}(t)$ and the noise variance σ^2. The ML estimates of these unknowns are calculated as the maximizing arguments of $L(\theta, \mathbf{s}(t), \sigma^2)$, the rationale being that these values make the probability of the observations as large as possible. For convenience, the ML estimates are alternatively defined as the minimizing arguments of the negative log-likelihood function $-\log L(\theta, \mathbf{s}(t), \sigma^2)$. Normalizing by N and ignoring the parameter-independent L log π-term, we get

$$l_{DML}(\theta, \mathbf{s}(t), \sigma^2) = L\log\sigma^2 + \frac{1}{\sigma^2 N}\sum_{t=1}^{N}\|\mathbf{x}(t) - \mathbf{A}\mathbf{s}(t)\|^2, \tag{47}$$

whose minimizing arguments are the deterministic maximum likelihood (DML) estimates.

As is well-known [15, 142], explicit minima with respect to σ^2 and $\mathbf{s}(t)$ are given by

$$\hat{\sigma}^2 = \frac{1}{L}\mathrm{Tr}\{\Pi_{\mathbf{A}}^{\perp}\hat{\mathbf{R}}\} \tag{48}$$

$$\hat{\mathbf{s}}(t) = \mathbf{A}^{\dagger}\mathbf{x}(t), \tag{49}$$

where $\hat{\mathbf{R}}$ is the sample covariance matrix, $\mathbf{A}^{\dagger}$ is the Moore-Penrose pseudo-inverse of $\mathbf{A}$ and $\Pi_{\mathbf{A}}^{\perp}$ is the orthogonal projector onto the nullspace of $\mathbf{A}^H$, i.e.,

$$\hat{\mathbf{R}} = \frac{1}{N}\sum_{t=1}^{N}\mathbf{x}(t)\mathbf{x}^H(t) \tag{50}$$

$$\mathbf{A}^{\dagger} = (\mathbf{A}^H\mathbf{A})^{-1}\mathbf{A}^H \tag{51}$$

$$\Pi_{\mathbf{A}} = \mathbf{A}\mathbf{A}^{\dagger} \tag{52}$$

$$\Pi_{\mathbf{A}}^{\perp} = \mathbf{I} - \Pi_{\mathbf{A}}. \tag{53}$$

Substituting Eqs. 48 and 49 into Eq. 46 shows that the DML signal parameter estimates are obtained by solving the following minimization problem:

$$\hat{\theta}_{DML} = \arg\left\{\min_{\theta}\mathrm{Tr}\{\Pi_{\mathbf{A}}^{\perp}\hat{\mathbf{R}}\}\right\}. \tag{54}$$

The interpretation is that the measurements $\mathbf{x}(t)$ are projected onto a model subspace orthogonal to all anticipated signal components, and a power measurement $\frac{1}{N}\sum_{t=1}^{N}\|\Pi_{\mathbf{A}}^{\perp}\mathbf{x}(t)\|^2 = \mathrm{Tr}\{\Pi_{\mathbf{A}}^{\perp}\hat{\mathbf{R}}\}$ is evaluated. The energy should clearly be smallest when the projector indeed removes all the true signal components, i.e., when $\theta = \theta_0$. Since only a finite number of noisy samples is available, the energy is not perfectly measured and $\hat{\theta}_{DML}$ will deviate from θ_0. However, if the scenario is stationary, the error will converge to zero as the number of samples is increased to infinity . This remains valid for correlated or even coherent signals, although the accuracy in finite samples is somewhat dependent upon signal correlations. Notice also that Eq. 54 reduces to the Bartlett beamformer in the case of a single source ($M = 1$).

To calculate the DML estimates, the non-linear M-dimensional optimization problem (Eq. 54) must be solved numerically. Finding the signal waveform and noise variance estimates (if desired) is then straightforward, by inserting $\hat{\theta}_{DML}$ into Eqs. 48-49. Given a good initial guess, a Gauss-Newton technique (see e.g. [24, 137]) usually converges rapidly to the minimum of Eq. 47. Obtaining sufficiently accurate initial estimates, however, is generally a computationally expensive task. If these are poor, the search procedure may converge to a local minimum, and never reach the desired global minimum. A spectral-based method is a natural choice for an initial estimator, provided all sources can be resolved. Another possibility is to apply the alternating projection technique of [162]. However, convergence to the global minimum can still not be guaranteed. Some additional results on the global properties of the criteria can be found in [90].

Stochastic Maximum Likelihood

The other ML technique reported in the literature is termed the stochastic maximum likelihood (SML) method. This method is obtained by modeling the signal waveforms as

Gaussian random processes. This model is reasonable, for instance, if the measurements are obtained by filtering wideband signals using a narrow bandpass filter. It is, however, important to point out that the method is applicable even if the data is not Gaussian. In fact, the asymptotic (for large samples) accuracy of the signal parameter estimates can be shown to depend only on the second-order properties (powers and correlations) of the signal waveforms [89, 115]. With this in mind, the Gaussian signal assumption is merely a way to obtain a tractable ML method. Let the signal waveforms be zero-mean with second-order properties

$$\mathrm{E}\{\mathbf{s}(t)\mathbf{s}^H(s)\} = \mathbf{P}\delta_{t,s} \tag{55}$$

$$\mathrm{E}\{\mathbf{s}(t)\mathbf{s}^T(s)\} = 0, \tag{56}$$

leading to the observation vector $\mathbf{x}(t)$ be a white, zero-mean and circularly symmetric Gaussian random vector with covariance matrix

$$\mathbf{R} = \mathbf{A}(\theta)\mathbf{P}\mathbf{A}^H(\theta) + \sigma^2\mathbf{I}. \tag{57}$$

The set of unknown parameters is, in this case, different from that in the deterministic signal model. The likelihood function now, depends on θ, $\mathbf{P}$ and σ^2. The negative log-likelihood function (ignoring constant terms) is in this case easily shown to be proportional to

$$\frac{1}{N}\sum_{t=1}^{N}\left\|\Pi_{\mathbf{A}}^{\perp}\mathbf{x}(t)\right\|^2 = \mathrm{Tr}\{\Pi_{\mathbf{A}}^{\perp}\hat{\mathbf{R}}\}. \tag{58}$$

Although this is a highly non-linear function, this criterion allows explicit separation of some of the parameters. For fixed θ, the minimum with respect to σ^2 and $\mathbf{P}$ can be shown to be [16, 57]

$$\hat{\sigma}^2_{SML}(\theta) = \frac{1}{L-M}\mathrm{Tr}\{\Pi_{\mathbf{A}}^{\perp}\} \tag{59}$$

$$\hat{\mathbf{P}}_{SML}(\theta) = \mathbf{A}^{\dagger}\left(\hat{\mathbf{R}} - \hat{\sigma}^2_{SML}(\theta)\mathbf{I}\right)\mathbf{A}^{\dagger H}. \tag{60}$$

With these estimates substituted into (58), the following compact form is obtained

$$\hat{\theta}_{SML} = \arg\left\{\min_{\theta}\log\left|\mathbf{A}\hat{\mathbf{P}}_{SML}(\theta)\mathbf{A}^H + \hat{\sigma}^2_{SML}(\theta)\mathbf{I}\right|\right\}. \tag{61}$$

In addition, this criterion has a nice interpretation, namely that the determinant, termed the *generalized variance* in the statistical literature, measures the volume of a confidence interval for the data vector. Consequently, we are looking for the model of the observations with the "lowest cost" and in harmony with the ML principle.

The criterion function in Eq. 61 is also a highly non-linear function of its argument θ. A Newton-type technique implementation of the numerical search is reported in [90] and an excellent statistical accuracy results when the global minimum is attained. Indeed, the SML signal parameter estimates have been shown to have a better large sample accuracy than the corresponding DML estimates [89, 115], with the difference being significant only for small numbers of sensors, low SNR and highly correlated signals. This property holds regardless of the actual distribution of the signal waveforms; in particular they need not be Gaussian. For Gaussian signals, the SML estimates attain the Cramér-Rao lower bound (CRB) on the estimation error variance, derived under the stochastic signal model. This follows from the general theory of ML estimation (see e.g. [130]), since all unknowns in the stochastic model are estimated consistently. This in contrast with the deterministic model for which the number of signal waveform parameters $\mathbf{s}(t)$ grows without bound, as the number of samples increases, implying that they cannot be consistently estimated. Hence, the general ML theory does not apply and the DML estimates do not attain the corresponding ("deterministic") CRB.

Subspace-Based Approximations

As noted previously, subspace-based methods offer significant performance improvements in comparison to conventional beamforming methods. In fact, the MUSIC method has been shown to yield estimates with a large-sample accuracy identical to that of the DML method, provided the emitter signals are uncorrelated [112]. However, the spectral-based methods usually exhibit a large bias in finite samples, leading to resolution problems. This problem is especially notable for high source correlations. Recently, parametric subspace-based methods that have the same statistical performance (both theoretically and practically) as the ML methods have been developed [116, 117, 136, 137]. The computational cost for these so-called *Subspace Fitting* methods is, however, less than for the ML ditto. As will be seen later, a computationally attractive implementation for the ubiquitous case of a uniform linear array, is known.

Recall the structure of the eigendecomposition of the array covariance matrix (Eq. 33),

$$\mathbf{R} = \mathbf{A}\mathbf{P}\mathbf{A}^H + \sigma^2\mathbf{I} \tag{62}$$

$$= \mathbf{U}_s\Lambda_s\mathbf{U}_s^H + \sigma^2\mathbf{U}_n\mathbf{U}_n^H \tag{63}$$

As previously noted, the matrices $\mathbf{A}$ and $\mathbf{U}_S$ span the same range space whenever $\mathbf{P}$ has full rank. In the general case, the number of signal eigenvectors in $\mathbf{U}_S$ equals M', the rank of $\mathbf{P}$. The matrix $\mathbf{U}_S$ will then span an M'-dimensional subspace of $\mathbf{A}$. This can easily be seen by first expressing the identity in (62) as $\mathbf{I} = \mathbf{U}_s\mathbf{U}_s^H + \mathbf{U}_n\mathbf{U}_n^H$. Cancelling the $\sigma^2\mathbf{U}_n\mathbf{U}_n^H$-term in (63) then yields

$$\mathbf{A}\mathbf{P}\mathbf{A}^H + \sigma^2\mathbf{U}_s\mathbf{U}_s^H = \mathbf{U}_s\Lambda_s\mathbf{U}_s^H. \tag{64}$$

Post-multiplying on the right by $\mathbf{U}_S$ (note that $\mathbf{U}_s^H\mathbf{U}_s = \mathbf{I}$) and re-arranging gives the relation

$$\mathbf{U}_s = \mathbf{AT}, \tag{65}$$

where $\mathbf{T}$ is the full-rank $M \times M'$ matrix

$$\mathbf{T} = \mathbf{PA}^H\mathbf{U}_s\left(\Lambda_s - \sigma^2\mathbf{I}\right)^{-1}. \tag{66}$$

The relation in Eq. 65 forms the basis for the *Signal Subspace Fitting* (SSF) approach. Since θ and $\mathbf{T}$ are unknown, it appears natural to search for the values that solve Eq. 65. The resulting θ will be the true DOAs (under general identifiability conditions [146]), whereas $\mathbf{T}$ is an uninteresting "nuisance parameter." If an estimate $\hat{\mathbf{U}}_s$ of $\mathbf{U}_S$ is used instead, there will be no such solution. In this case, one attempts to minimize some distance measure between $\hat{\mathbf{U}}_s$ and $\mathbf{AT}$. For this purpose, the Frobenius norm turns out to be a useful measure, and when squared, it can be conveniently expressed as the sum of the squared Euclidean norms of the rows or columns. In light of this formulation, the connection to standard least-squares estimators is made clear. The SSF estimate is obtained by solving the following non-linear optimization problem:

$$\left\{\hat{\theta}, \hat{\mathbf{T}}\right\} = \arg\min_{\theta,\mathbf{T}} \left\|\hat{\mathbf{U}}_s - \mathbf{AT}\right\|_F^2. \tag{67}$$

Similar to the DML criterion (Eq. 47), this is a separable nonlinear least squares problem [47]. The solution for the linear parameter $\mathbf{T}$ (for fixed unknown $\mathbf{A}$) is

$$\hat{\mathbf{T}} = \mathbf{A}^{\dagger}\hat{\mathbf{U}}_s, \tag{68}$$

which, when substituted into Eq.67, leads to the concentrated criterion function

$$\hat{\theta} = \arg\left\{\min_{\theta} \mathrm{Tr}\left\{\Pi_{\mathbf{A}}^{\perp}\hat{\mathbf{U}}_s\hat{\Lambda}_s\hat{\mathbf{U}}_s^H\right\}\right\}. \tag{69}$$

Since the eigenvectors are estimated with a quality, commensurate with the closeness of the corresponding eigenvalues to the noise variance, it is natural to introduce a weighting of the eigenvectors and arrive at

$$\hat{\theta}_{SSF} = \arg\left\{\min_{\theta} \mathrm{Tr}\left\{\Pi_{\mathbf{A}}^{\perp}\hat{\mathbf{U}}_s\mathbf{W}\hat{\mathbf{U}}_s^H\right\}\right\}. \tag{70}$$

A natural question which arises is how to pick $\mathbf{W}$ to maximize the accuracy, i.e., to minimize the estimation error variance. It can be shown that the projected eigenvectors $\Pi_{\mathbf{A}}^{\perp}(\theta_0)\hat{\mathbf{u}}_k, k = 1,\ldots,M'$ are asymptotically independent. Hence, following from the theory of weighted least squares, [46], $\mathbf{W}$ should be a diagonal matrix containing the inverse of the covariance matrix of $\Pi_{\mathbf{A}}^{\perp}(\theta_0)\hat{\mathbf{u}}_k, k = 1,\ldots,M'$. This leads to the choice [117, 136]

$$\mathbf{W}_{opt} = \left(\Lambda_s - \sigma^2\mathbf{I}\right)^2\Lambda_s^{-1}. \tag{71}$$

Since $\mathbf{W}_{opt}$ depends on unknown quantities, we use instead

$$\hat{\mathbf{W}}_{opt} = \left(\hat{\Lambda}_s - \hat{\sigma}^2\mathbf{I}\right)^2\hat{\Lambda}_s^{-1}, \tag{72}$$

where $\hat{\sigma}^2$ denotes a consistent estimate of the noise variance, for example the average of the $L - M'$ smallest eigenvalues. The estimator defined by (70) with weights given by (72) is termed the *Weighted Subspace Fitting* (WSF) method. It has been shown to theoretically yield the same large sample accuracy as the SML method, and at a lower computational cost provided a fast method for computing the eigendecomposition is used. Practical evidence, e.g., [90], have given by hand that the WSF and SML methods also exhibit similar small sample (i.e. threshold) behaviour.

An alternative subspace fitting formulation is obtained by instead starting from the "MUSIC relation"

$$\mathbf{A}^H(\theta)\mathbf{U}_n = 0 \quad \text{if} \quad \theta = \theta_0, \tag{73}$$

which holds for $\mathbf{P}$ having full rank. Given an estimate of $\mathbf{U}_n$, it is natural to look for the signal parameters which minimize the following *Noise Subspace Fitting* (NSF) criterion,

$$\hat{\theta} = \arg\left\{\min_{\theta} \mathrm{Tr}\left\{\mathbf{A}^H\hat{\mathbf{U}}_n\hat{\mathbf{U}}_n^H\mathbf{AV}\right\}\right\}, \tag{74}$$

where $\mathbf{V}$ is some positive (semi-)definite weighting matrix. Interestingly enough, the estimates calculated by Eqs. 70 and 74 asymptotically coincide, if the weighting matrices are (asymptotically) related by [90]

$$\mathbf{V} = \mathbf{A}^{\dagger}(\theta_0)\hat{\mathbf{U}}_s\mathbf{W}\hat{\mathbf{U}}_s^H\mathbf{A}^{\dagger *}(\theta_0). \tag{75}$$

Note also that the NSF method reduces to the MUSIC algorithm for $\mathbf{V} = \mathbf{I}$, provided $\|\mathbf{a}(\theta)\|$ is independent of θ. Thus, in a sense the general estimator in Eq. 74 unifies the parametric methods and also encompasses the spectral-based subspace methods.

The NSF method has the advantage that the criterion function in Eq. 74 is a quadratic function of the steering matrix $\mathbf{A}$. This is useful if any of the parameters of $\mathbf{A}$ enter linearly. An analytical solution with respect to these parameters is then readily available (see e.g., [138]). However, this only happens in very special situations, rendering this forementioned advantage of limited importance. The NSF formulation is also fraught with some drawbacks, namely that it cannot produce reliable estimates for coherent signals, and that the optimal weighting $\mathbf{V}_{opt}$ depends on θ_0, so that a two-step procedure has to be adopted.

Uniform Linear Arrays

The steering matrix for a uniform linear array has a very special, and as it turns out, useful structure. From Eq. 28, the ULA steering matrix takes the form

$$\mathbf{A}(\theta)=\begin{bmatrix} 1 & 1 & \cdots & 1 \\ e^{j\phi 1} & e^{j\phi 2} & \cdots & e^{j\phi M} \\ \vdots & \vdots & & \vdots \\ e^{j(L-1)\phi 1} & e^{j(L-1)\phi 2} & \cdots & e^{j(L-1)\phi M} \end{bmatrix}. \tag{76}$$

This structure is referred to as a *Vandermonde matrix.* (Each component of a column of a Vandermonde matrix is an integer power of the first component, and the integer coincides with its row number.) [47].

Root-MUSIC

The Root-MUSIC method [11], as the name implies, is a polynomial-rooting version of the previously described MUSIC technique. The idea dates back to Pisarenko's method [94]. Let us define the polynomials

$$p_l(z)=\mathbf{u}_l^H\mathbf{p}(z),\ l=M+1,M+2,\ldots,L, \tag{77}$$

where $\mathbf{u}_l$ is the *l:th* eigenvector of $\mathbf{R}$ and

$$\mathbf{p}(z)=\left[1,z,\ldots,z^{L-1}\right]^T \tag{78}$$

From our problem formulation, one makes the basic observation that $p_l(z)$ has M of its zeros at $e^{j\phi m}$, m = 1,2,..., M, provided that $\mathbf{P}$ has full rank. To exploit the information from all noise eigenvectors simultaneously, we want to find the zeros of the MUSIC-like function

$$\mathbf{p}^H(z)\hat{\mathbf{U}}_n\hat{\mathbf{U}}_n^H\mathbf{p}(z). \tag{79}$$

However, the latter is not a polynomial in z (note that powers of z^* are now present), which complicates the search for zeros. Since the values of z on the unit circle are of interest, we can use $\mathbf{p}^T(z^{-1})$ for $\mathbf{p}^H(z)$, which gives the Root-MUSIC polynomial

$$p(z)=z^{L-1}\mathbf{p}^T\left(z^{-1}\right)\hat{\mathbf{U}}_n\hat{\mathbf{U}}_n^H\mathbf{p}(z). \tag{80}$$

Note that $p(z)$ is a polynomial of degree $2(L-1)$, whose roots occur in mirrored pairs with respect to the unit circle. Of the ones inside, the phases of the M that have the largest magnitude, say $\hat{z}_1,\hat{z}_2,\ldots,\hat{z}_M$,yield the DOA estimates, as

$$\hat{\theta}_m=\arccos\left(\frac{1}{kd}\arg\{\hat{z}_m\}\right),\ m=1,2,\ldots,M. \tag{81}$$

It has been shown [112, 113] that MUSIC and Root-MUSIC have identical asymptotic properties, although in small samples Root-MUSIC has empirically been found to perform significantly better. As previously alluded to, this can be attributed to a larger bias of estimates for spectral-based methods, as compared to the parametric techniques [69, 98].

ESPRIT

The ESPRIT algorithm [93, 101] uses the structure of the ULA steering vectors in a slightly different way. The observation here is that $\mathbf{A}$ has a so-called *shift structure*. Define the sub-matrices $\mathbf{A}_1$ and $\mathbf{A}_2$ by deleting the first and last rows from $\mathbf{A}$ (defined in (13)) respectively, i.e.,

$$\mathbf{A}=\begin{bmatrix}\mathbf{A}_1\\ \text{last row}\end{bmatrix}=\begin{bmatrix}\text{first row}\\ \mathbf{A}_2\end{bmatrix}. \tag{82}$$

By the structure of Eq. 76, $\mathbf{A}_1$ and $\mathbf{A}_2$ are related by the formula

$$\mathbf{A}_2=\mathbf{A}_1\Phi, \tag{83}$$

where Φ is a diagonal matrix having the roots $e^{j\phi m}$, m = 1,2,..., M, on the diagonal. Thus, the DOA estimation problem can be reduced to that of finding Φ. Analogously to the other subspace-based algorithms, ESPRIT relies on properties of the eigendecomposition of the array covariance matrix. Applying this deletion transformation to Eq. (65), we get

$$\mathbf{U}_1=\mathbf{A}_1\mathbf{T}\ ,\ \mathbf{U}_2=\mathbf{A}_2\mathbf{T}, \tag{84}$$

where $\mathbf{U}_S$ has been partitioned conformably with $\mathbf{A}$ into the sub-matrices $\mathbf{U}_1$ and $\mathbf{U}_2$. Combining (83) and (84) yields

$$\mathbf{U}_2=\mathbf{A}_1\Phi\mathbf{T}\ ,\ \mathbf{U}_1=\mathbf{T}^{-1}\Phi\mathbf{T}, \tag{85}$$

which, by defining $\Psi=\mathbf{T}^{-1}\Phi\mathbf{T}$, becomes

$$\mathbf{U}_2=\mathbf{U}_1\Psi. \tag{86}$$

Note that Ψ and Φ are related by a similarity transformation, and hence have the same eigenvalues. The latter is of course given by $e^{j\phi m}$, m = 1,2,..., M, and are related to the DOAs as in Eq. 81. The ESPRIT algorithm is now stated:

1. Compute the eigendecomposition of the array covariance matrix $\hat{\mathbf{R}}$
2. Form $\hat{\mathbf{U}}_1$ and $\hat{\mathbf{U}}_2$ from the M principal eigenvectors
3. Solve the approximate relation Eq. 86 in either a Least-Squares sense (LS-ESPRIT) or a Total-Least-Squares [46, 47] sense (TLS-ESPRIT)
4. The DOA estimates are obtained by applying the inversion formula Eq. 81 to the eigenvalues of $\hat{\Psi}$

It has been shown that LS-ESPRIT and TLS-ESPRIT yield identical asymptotic estimation accuracy [97], although in small samples TLS-ESPRIT usually has an edge. In addition, unlike LS-ESPRIT, TLS-ESPRIT accounts for the noisy nature of both $\hat{\mathbf{U}}_1$ and $\hat{\mathbf{U}}_2$ which is more intuitively appealing. Note also that the ESPRIT algorithm allows more flexibility

in partitioning of the array (or of the **A** matrix), so long as a shift structure can be obtained and subsequently estimated.

IQML and Root-WSF

Another interesting exploitation of the ULA structure was presented in [19], although the idea can be traced back to the Steiglitz and McBride algorithm for system identification [111]. The IQML (Iterative Quadratic Maximum Likelihood) algorithm is an iterative procedure for minimizing the DML criterion

$$V(\theta) = \mathrm{Tr}\left\{\Pi_{\mathbf{A}}^{\perp}\hat{\mathbf{R}}\right\}. \tag{87}$$

The idea is to re-parameterize the projection matrix $\Pi_{\mathbf{A}}^{\perp}$ using a basis for the nullspace of $\mathbf{A}^H$. Towards this end, one defines a polynomial $b(z)$ to have its M roots at $e^{j\phi m}$, $m = 1,2,\ldots, M$, i.e.,

$$b(z) = z^M + b_1 z^{M-1} + \cdots + b_M = \prod_{m=1}^{M}\left(z - e^{j\phi m}\right) \tag{88}$$

Then, by construction the following relation holds true

$$\begin{bmatrix} b_M & b_{M-1} & \cdots & 1 & \cdots & 0 \\ & \ddots & \ddots & & \ddots & \\ 0 & & b_M & b_{M-1} & \cdots & 1 \end{bmatrix} \begin{bmatrix} 1 & \cdots & 1 \\ e^{j\phi 1} & \cdots & e^{j\phi M} \\ \vdots & \vdots & \vdots \\ e^{j(L-1)\phi 1} & \cdots & e^{j(L-1)\phi M} \end{bmatrix} = 0 \tag{89}$$

$$\Leftrightarrow \mathbf{B}^H\mathbf{A} = 0.$$

Since **B** has a full rank of $L - M$, its columns do in fact form a basis for the nullspace of $\mathbf{A}^H$. Clearly the orthogonal projections onto these subspaces must coincide, implying

$$\Pi_{\mathbf{A}}^{\perp} = \mathbf{B}\left(\mathbf{B}^H\mathbf{B}\right)^{-1}\mathbf{B}^H. \tag{90}$$

Now the DML criterion function can be parameterized by the polynomial coefficients b_k in lieu of the DOAs θ_k. The DML estimate (54) can be calculated by solving

$$\hat{\mathbf{b}} = \arg\min_{\mathbf{b}} \mathrm{Tr}\left\{\mathbf{B}\left(\mathbf{B}^H\mathbf{B}\right)^{-1}\mathbf{B}^H\hat{\mathbf{R}}\right\} \tag{91}$$

and then applying Eq. 81 to the roots of the estimated polynomial. Unfortunately, Eq. 91 is still a difficult non-linear optimization problem. However, [19] suggested an iterative solution as follows

1. Set $\mathbf{U} = \mathbf{I}$
2. Solve the quadratic problem

$$\hat{\mathbf{b}} = \arg\min_{\mathbf{b}} \mathrm{Tr}\left\{\mathbf{B}\mathbf{U}\mathbf{B}^H\hat{\mathbf{R}}\right\} \tag{92}$$

3. Form $\hat{\mathbf{B}}$ and put $\mathbf{U} = \left(\hat{\mathbf{B}}^H\hat{\mathbf{B}}\right)^{-1}$
4. Check for convergence. If not, goto Step 2
5. Apply (81) to the roots of $\hat{b}(z)$

Since the roots of $b(z)$ should be on the unit circle, [20] suggested using the constraint

$$b_m = b_{M-m}^H,\ m = 1,2,\ldots,M \tag{93}$$

when solving Eq. 92. Now, Eq. 93 does not guarantee unity magnitude roots, but it can be shown that the accuracy loss due to this fact is negligible. While the above described IQML algorithm cannot be guaranteed to converge, it has indeed been found to perform well in simulations.

An improvement over IQML was introduced in [116]. The idea is simply to apply the IQML iterations to the WSF criterion Eq. 70. Since the criteria have the same form, the modification is straightforward. However, there is a very important advantage of using the rank-truncated form $\hat{\mathbf{U}}_s\mathbf{W}\hat{\mathbf{U}}_s^H$ rather than $\hat{\mathbf{R}}$ in Eq. 92, with **W** as defined in Eq. 72. That is, after the second pass of the iterative scheme, the estimates already have the asymptotic accuracy of the true optimum! Hence, the resulting Root-WSF algorithm is no longer an iterative procedure:

1. Solve the quadratic problem

$$\hat{\mathbf{b}} = \arg\min_{\mathbf{b}} \mathrm{Tr}\left\{\mathbf{B}\mathbf{B}^H\hat{\mathbf{U}}_s\mathbf{W}\hat{\mathbf{U}}_s^H\right\} \tag{94}$$

2. Solve the quadratic problem

$$\hat{\mathbf{b}} = \arg\min_{\mathbf{b}} \mathrm{Tr}\left\{\mathbf{B}\left(\hat{\mathbf{B}}^H\hat{\mathbf{B}}\right)^{-1}\mathbf{B}^H\hat{\mathbf{U}}_s\mathbf{W}\hat{\mathbf{U}}_s^H\right\} \tag{95}$$

3. Apply (81) to the roots of $\hat{b}(z)$.

Note that this algorithm is essentially in closed form (aside from the eigendecomposition and polynomial rooting), and that the resulting estimates have the best possible asymptotic accuracy. Thus, the Root-WSF algorithm is a strong candidate for the "best" method for ULAs.

Additional Topics

The emphasis in this paper is on parameter estimation methods in sensor array processing. Because of space limitations, we have clearly omitted several interesting issues from the main discussion. To partially fill the gap, a very brief overview of these additional topics is given in the following. We structure this section in the form of a commented enumeration of references to selected specialized papers.

Number of Signals Estimation

In applications of model-based methods, an important problem is the determination of M, the number of signals. In the case of non-coherent signals, the number of signals is equal to the number of "large" eigenvalues of the array covariance matrix. This fact is used to obtain relatively simple non-parametric algorithms for determining M. The most frequently used approach emanates from the factor analysis literature

[4]. The idea is to determine the multiplicity of the smallest eigenvalue, which theoretically equals $L - M$. A statistical hypothesis test is proposed in [105], whereas [144, 161] are based on information theoretic criteria, such as Akaike's AIC (an information theoretic criterion) and Rissanen's MDL (minimum description length). Unfortunately, the aforementioned approach is very sensitive to the assumption of a spatially white noise field [157]. An alternative idea based on using the eigenvectors rather than the eigenvalues is pursued in the referenced paper. Another non-parametric method is presented in [31].

In the presence of coherent signals, the methods as just stated will fail, since the dimension of the signal subspace is in this case smaller than M. However, for ULAs one can test the eigenvalues of the spatially smoothed array covariance matrix to determine M as proposed in [108] and improved by [68].

A more systematic approach to estimating the number of signals is possible if the maximum likelihood estimator is employed. A classical generalized likelihood ratio test (GLRT) is described in [90], whereas [143] presents an information theoretic approach. Another model-based detection technique is presented in [90, 137], based on the weighted subspace fitting method. For determining the number of signals the model-based methods require signal parameter estimates for an increasing hypothesized number of signals, until some pre-specified criterion is met. The approach is thus inherently more computationally intensive than the non-parametric tests. Its performance in difficult signal scenarios is, however, improved and is in addition less sensitive to small perturbations of the assumed noise covariance matrix.

Reduced Dimension Beamspace Processing

At the exception of the beamforming-based methods, the estimation techniques discussed herein require that the outputs of all elements of the sensor array be available in digital form. In many applications, the required number of high-precision receiver front-ends and A/D converters may be prohibitive. Arrays of 10^4 elements are not uncommon, for example in radar applications. Techniques for reducing the dimensionality of the observation vector with minimal effect on performance, are therefore of great interest. As already discussed previously, a useful idea is to employ a linear transformation

$$\mathbf{z}(t) = \mathbf{T}^{*}\mathbf{x}(t), \tag{96}$$

where $\mathbf{T}$ is L R, with (usually) $R << L$. The transformation is typically implemented in analog hardware, thus significantly reducing the number of required A/D converters. The reduced-dimension observation vector $\mathbf{z}(t)$ is usually referred to as the *beamspace* data, and $\mathbf{T}$ is a *beamspace transformation*.

Naturally, processing the beamspace data significantly reduces the computational load of the digital processor. However, reducing the dimension of the data also implies a loss of information. The beamspace transformation can be thought of as a multichannel beamformer. By designing the beamformers (the columns of $\mathbf{T}$) so that they focus on a relatively narrow DOA sector, the essential information in $\mathbf{x}(t)$ regarding sources in that sector can be retained in $\mathbf{z}(t)$. See e.g., [41, 134, 159, 165] and the references therein. With further *a priori* information on the locations of sources, the beamspace transformation can in fact be performed with no loss of information [5]. As previously alluded to, beamspace processing can even *improve* the resolution (the bias) of spectral-based methods.

Note that the beamspace transformation effectively changes the array propagation vectors from $\mathbf{a}(\theta)$ into $\mathbf{T}^{*}\mathbf{a}(\theta)$. It is possible to utilize this freedom to give the beamspace array manifold a simpler form, such as that of a ULA, [43]. Hence, the computationally efficient ULA techniques are applicable in beamspace. In [82], a transformation that maps a uniform circular array into a ULA is proposed and analyzed, enabling computationally efficient estimation of both azimuth and elevation.

Estimation Under Model Uncertainty

As implied by the terminology, model-based signal processing relies on the availability of a precise mathematical description of the measured data. When the model fails to reflect the physical phenomena with a sufficient accuracy, the performance of the methods will clearly degrade. In particular, deviations from the assumed model will introduce bias in the estimates, which for spectral-based methods is manifested by a loss of resolving power and a presence of spurious peaks. In principle, the various sources of modeling errors can be classified into noise covariance and array response perturbations.

In many applications of interest, such as communication, sonar and radar, the background noise is dominated by man-made noise. While the noise generated in the receiving equipment is likely to fulfill the spatially white assumption, the man-made noise tends to be quite directional. The performance degradation under noise modeling errors is studied in, e.g. [77, 140]. One could in principle envision extending the model-based estimation techniques to also include estimation of the noise covariance matrix. Such an approach has the potential of improving the robustness to errors in the assumed noise model [143, 152]. However, for low SNR's, this solution is less than adequate. The simultaneous estimation of a completely unknown noise covariance matrix and of the signal parameters poses a problem unless some additional information which enables us to separate signal from noise, is available. It is, for example, always possible to infer that the received data is nothing but noise, and that the (unknown) noise covariance matrix is precisely the observed array sample covariance matrix. Estimation of parametric (structured) noise models is considered in, e.g., [18, 64]. So-called instrumental variable techniques are proposed, e.g. in [119] (based on assumptions on the temporal correlation of signals and

noise) and [153] (utilizing assumptions on the spatial correlation of the signals and noise). Methods based on other assumptions appeared in [92, 131].

At high SNR, the modeling errors are usually dominated by errors in the assumed signal model. The signals have a non-zero bandwidth, the sensor positions may be uncertain, the receiving equipment may not be perfectly calibrated, etc. The effects of such errors are studied e.g. in [42, 76, 125, 126]. In some cases it is possible to physically quantify the error sources. A "self-calibrating" approach may then be applicable [100, 138, 147], albeit at quite a computational cost. In [125, 126, 139], robust techniques for unstructured sensor modeling errors are considered.

Wideband Data Processing

The methods presented herein are essentially limited to processing narrowband data. In many applications (e.g. radar and communication), this is indeed a realistic assumption. However, in other cases (e.g. sonar), the received signal may be broadband. A natural extension of all these methods is to employ narrowband filtering, for example using the Fast Fourier Transform (FFT). An optimal exploitation of the data entails combining information from different frequency bins [66], see also [145]. A simpler suboptimal approach is to process the different FFT channels separately using a standard narrowband method, whereafter the DOA estimates at different bins must be combined in some appropriate way.

Another approach is to explicitly model the array output as a multidimensional time series, using an autoregressive moving average (ARMA) model. The poles of the system are estimated, e.g. using the overdetermined Yule-Walker equations. A narrowband technique can subsequently be employed using the estimated spectral density matrix, evaluated at the system poles. In [122], the MUSIC algorithm is applied, whereas [88] proposes to use the ESPRIT algorithm.

A wideband DOA estimation approach inspired by beamspace processing is the so-called coherently averaged signal subspace method, originally introduced in [141]. The idea is to first estimate the signal subspace at a number of FFT channels. The information from different frequency bins is subsequently merged by employing linear transformations. The objective is to make the transformed steering matrices $\mathbf{A}$ at different frequencies as identical as possible, for example by focusing at the center frequency of the signals. See, e.g. [56, 71, 109] for further details.

Fast Subspace Calculation and Tracking

The implementation of subspace-based methods in applications with real-time operation usually experiences a bottleneck in the calculation of the signal subspace. A scheme for fast computation of the signal subspace is proposed in [60], and methods for subspace tracking are considered in [30]. The idea is to exploit the "low-rank plus $\sigma^2\mathbf{I}$" structure of the ideal array covariance matrix. An alternative gradient-based technique for subspace tracking is proposed in [160]. Therein, it is observed that the solution $\mathbf{W}$, of the constrained optimization problem,

$$\max_{\mathbf{W}} \mathrm{Tr}\left\{\mathbf{W}^*\hat{\mathbf{R}}\mathbf{W}\right\} \quad \text{subject to } \mathbf{W}^*\mathbf{W} = \mathbf{I}$$

spans the signal subspace.

For some methods, estimates of the individual principal eigenvectors are required, in addition to the subspace they span. A number of different methods for eigenvalue/vector (The referenced paper considers tracking of the principal left singular values of the data matrix. Mathematically, but perhaps not numerically, these are identical to the eigenvectors of the sample covariance matrix.) tracking is given in [28]. A more recent approach based on exploiting the structure of the ideal covariance is proposed and analyzed in [155]. The so-called fast subspace decomposition (FSD) technique is based on a Lanczos method for calculating the eigendecomposition. It is observed that the Lanczos iterations can be prematurely terminated without any significant performance loss.

Signal Structure Methods

Most "standard" approaches to array signal processing make no use of any available information about the signal structure. However, many man-made signals have a rich structure that can be used to improve the estimator performance. In digital communication applications, the transmitted signals are often *cyclostationary*, which implies that their autocorrelation functions are periodic. This additional information is exploited in e.g. [1, 154, 194], and algorithms for DOA estimation of cyclostationary signals are derived and analyzed. In this approach, the wideband signals are easily incorporated into the framework, and the number of signals may exceed the number of sensors with the provision that they do not all share the same cyclic frequency (which refers to the frequency at which the spatial correlation function repeats itself).

A different approach utilizing signal structure is based on high-order statistics. As is well-known, all information about a Gaussian signal is conveyed in the first and second order moments. However, for non-Gaussian signals, there is potentially more to be gained by using higher moments. This is particularly so if the noise can be regarded as Gaussian. Then, the high-order cumulants will be theoretically noise-free, as they vanish for Gaussian signals. Methods based on fourth-order cumulants are proposed in [26, 95], whereas [107] proposes to use high-order cyclic spectra (for cyclostationary signals).

A common criticism of both approaches (those based on cyclostationarity and those based on high-order statistics) is that they require a considerable amount of data to yield reliable results. This is due to the slower convergence of the estimated cyclic and high-order moments to their theoretical values as the number of data is increased compared to that of second order moments.

Polarization Sensitivity

Most antenna arrays used in electro-magnetic applications are sensitive to polarization differences among the received signals. Recall that the wave equation (7) is in fact vector-valued, and that a similar equation holds for the magnetic components. Provided that each polarization component can be calibrated separately, the signal polarization can be utilized for improving the DOA estimation performance, even if the array only measures the sum of the polarization components. An extension of the MUSIC method to polarization sensitive arrays is proposed in [39], whereas [78, 127, 163] consider parametric methods. In [148], it is shown that polarization diversity can also significantly improve the signal waveform estimates, a fact which has long been known in microwave communications and which could be of considerable interest in array processing applications, e.g. communication applications.

A more complete signal model is considered in [54, 86]. Therein, it is assumed that the receiving sensors measure all six field components of the electric and magnetic fields. This allows source localization using only one so-called *vector sensor*.

Time Series Analysis

The DOA estimation problem employing a ULA shares some common aspects with time series analysis. Indeed, an important pre-cursor of the MUSIC algorithm is Pisarenko's method [94] for estimation of the frequencies of damped/undamped sinusoids in noise, whose covariance function measurements are given. Similarly, Kung's algorithm for state-space realization of a measured impulse response [73] is an early version of the ESPRIT algorithm. An important difference between the time series case and the (standard) DOA estimation problem is that the time series data is usually estimated using a sliding window. A "sensor array-like data vector" $\mathbf{x}(t)$ is formed from the scalar time series $y(t)$ by using

$$\mathbf{x}(t) = \left[y(t), y(t+1), \ldots y(t+L-1)\right]^T.$$

The windowing transformation induces a temporal correlation in the L-dimensional time series $\mathbf{x}(t)$, even if the scalar process $y(t)$ is temporally white. This fact complicates the analysis, as in the case of spatial smoothing in DOA estimation, see e.g. [27, 68, 188]. A further complication arises in time series analysis problems when there is a known input signal present. This problem has fortunately, also been successfully tackled using ideas from sensor array signal processing [135].

Applications

The research progress of parameter estimation and detection in array processing has resulted in a great diversity of applications, and continues to provide fertile ground for new ones. In this section we discuss three important application areas.

Personal Communications

Receiving arrays and related estimation/detection techniques have long been used in High Frequency communications. These applications have recently reemerged and received a significant attention by researchers, as a potentially useful "panacea" for numerous problems in personal communications (see e.g., [3, 120, 123, 151]). They are expected to play a key role in accommodating a multiuser communication environment, subject to severe multipath.

One of the most important problems in a multiuser asynchronous environment is the inter-user interference, which can degrade the performance quite severely. This is also the case in a practical Code-Division Multiple Access (CDMA) system, because the varying delays of different users induce non-orthogonal codes. An interesting application of the MUSIC algorithm for estimating these propagation delays is presented in [121]. The base stations in mobile communication systems have long been using *spatial diversity* for combating fading due to the severe multipath. However, using an antenna array of several elements introduces additional degrees of freedom, which can be used to obtain higher selectivity. An adaptive receiving array can be steered in the direction of one user at a time, while simultaneously nulling interference from other users, much in the the same way as the beamforming techniques described previously.

The multipath which may be caused by buildings reflections or hills, etc. introduces difficulties for conventional adaptive array processing. Undesired cancelation may occur [149], and spatial smoothing may be required to achieve a proper selectivity. In [3], it is proposed to identify all signal paths emanating from each user, whereafter an optimal signal combination is performed. A configuration equivalent to the beamspace array processing with a simple energy differencing scheme serves in localizing incoming users waveforms [103]. This beamspace strategy underlies an adaptive optimization technique proposed in [120], which addresses the problem of mitigating the effects of dispersive time varying channels.

Communication signals have a rich structure that can be exploited for signal separation using antenna arrays. Indeed, the DOAs need not be estimated. Instead, signal structure methods such as the constant-modulus beamformer [48] have been proposed for directly estimating the steering vectors of the signals, thereby allowing for *blind* (i.e., not requiring a training sequence) signal separation. Techniques based on combining beamforming and demodulation of digitally modulated signals have also recently been proposed (see [80, 100, 128, 129]). It is important to note that the various optimal and/or suboptimal proposed methods are of current research interest, and that in practice, many challenging and interesting problems remain to be addressed.

Radar and Sonar

The classical application of array signal processing is in radar and sonar, and modern model-based techniques have also

found their way to these areas [34, 51, 52, 79, 91]. The antenna array is, for example, used for source localization, interference cancelation and ground clutter suppression.

In radar applications, the mode of operation is referred to as active. This is on account of the role of the antenna array based system which radiates pulses of electro-magnetic energy and listens for the return. The parameter space of interest may vary according to the geometry and sophistication of the antenna array. The radar returns enable estimation of parameters such as velocity (Doppler frequency), range and DOAs of targets of interest [130]. Using passive far-field listening arrays, only the DOAs can be estimated.

In sonar applications, on the other hand, the signal energy is usually acoustic, and measured using arrays of hydrophones. The sonar can operate in an active as well as passive mode. In a passive mode, the receiving array has the capability of detecting and locating distant sources. Deformable array models are often used in sonar, as the receiving antenna is typically towed under water [79]. Techniques with piecewise linear subarrays are used in the construction of the overall solution. Recent experimental results using passive sonar and also seismic (seismometer) arrays are presented in [17].

In an active mode, a sonar system emits acoustic (electromagnetic arrays are also used underwater) energy and monitors and retrieves any existing echo. This again can be used for parameter estimation, such as bearings and velocity etc., using the delay of the echo. Despite its limitations due to the bending speed-of-propagation profiles and the high propagation losses, sonar together with related estimation techniques, remains a reliable tool for range, bearing estimation and other imaging tasks in underwater applications. However, the difficult propagation conditions under water may call for more complex signal modeling, such as in *matched field processing* (see e.g. [10]).

Industrial Applications

Sensor array signal processing techniques have drawn much interest from industrial applications, such as manufacturing and medical applications. In medical imaging and hyperthermia treatment [37, 38], circular arrays are commonly used as a means to focus energy in both an injection mode as well as reception mode. It has also been used in treatment of tumors [36]. In electrocardiograms, planar arrays are used to track the evolution of wavefronts which in turn provide information about the condition of a patient's heart. Array processing methods have also been adopted to localize brain activity using biomagnetic sensor arrays, so-called super-conducting quantum interference device (SQUID) magnetometers [85]. It is expected that the medical applications will proliferate as more resolution is sought, e.g. signals emanating from a womb may be of more interest than those of a mother.

Other applications in industry are almost exclusively in automatic monitoring and fault detection/localization. In engines, sensors are placed in a judicious and convenient way to detect and potentially localize faults such as knocks or broken gears [49, 166]. Another emerging and important application of array signal processing is in using notions from optics to carry out tasks in product quality assurance in a manufacturing environment [2], and in object shape characterization in tomography [83, 84]. An example is provided in "Radar Example."

Future Directions

In summary, and as demonstrated by the above applications which are more or less advanced in their stage of investigation, new connections of certain problems (new or old) keep being made to array processing methods whose resolving power, in turn, provides in many cases a superb improvement over more conventional solutions. It is clear that the theoretical interest in sensor array processing has somewhat diminished in recent years, and is largely due to the lag of applications. However, we believe that the future holds nice surprises as the applications are catching up with the theoretical foundations, and new perspectives from fields such as geometry of polynomials and other insights from communications (e.g. equalization) start making inroads into the research community. It is our belief that we will be witnessing an explosive development of array processing algorithms within personal communications, as the various network operators start demanding smart antennas (which already happened). We also look forward to more impact of model-based array signal processing in various imaging problems, where more traditional approaches dominate at present. Examples include synthetic aperture radar (SAR) and underwater acoustic imaging. The interest in remote sensing and imaging is expected to grow, particularly on account of the applications in environmental studies. Other "unexpected" environmental applications have also recently appeared, such as chemical sensor arrays [87].

Measured Data Experiment

In this section, the viability of the various methods is tested on experimental data. In the first example, the results using radar data are presented in some detail, whereas the second example uses image data.

Radar Example

The receiver is an $L = 32$-element uniform linear array, which is mounted vertically so that the DOA is in this case the elevation angle. With reference to Figure 1, we will assume that the array is mounted along the y-axis, so that $\theta = 0$ corresponds to the array broadside. The sensors have a horizontal polarization. The array is located on the shore of Lake Huron, whereas the transmitter is on the opposite side. Thus, the surface of the lake will ideally generate a specular multipath component. There will most likely also be a diffuse multipath. The data collection system, referred to as the Multi-Parameter Adaptive Radar System (MARS), was developed at the Communications Research Laboratory at

McMaster University. More details of the MARS system and the experimental conditions can be found in [32]. The particular data sets used herein were also employed by Zoltowski [164], who obtained good results with a maximum-likelihood technique operating on beamspace data. The major goal herein is to investigate the achievable performance of "standard" DOA estimation methods on experimental data. A beamspace implementation is also considered.

Five data sets labeled **l41** through **l45** were available. Each set consists of a total of 127 snapshots, sampled at baseband with a sampling rate of 62.5 Hz. Due to potentially non-stationary conditions, the data set were divided into 8 batches, each comprising $N = 16$ snapshots, before further processing. The theoretical DOAs of the direct and reflected signal paths are fixed (at θ_1=0.0835° and θ_2=-0.303° respectively), but the carrier frequency varies between 8.62 GHz and 12.34 GHz. This causes the electrical angle separation to vary between $\Delta\phi = BW/3$ and $\Delta\phi = BW/2$, where $BW = 2\pi/L$ represents the standard beamwidth of the array (in radians). Note that the electrical angle for this setup is defined as

$$\phi = -kd\sin\theta,$$

because the DOA is defined relative to the array broadside. The given five data sets were processed using the previously described methods assuming a perfect ULA array response (Eq. 28), given that the array is quite carefully calibrated. As in any real data experiment, there are many possible sources of errors. The most obvious in this case, is the diffuse multipath, which may be modeled as a spatially extended emitter, the waveform of which probably has some correlation with that of the more point-like signal paths. To illustrate the problem, the eigenvalues of a typical sample covariance are depicted in Fig. 7, along with a realization from the theoretical model with two point sources in spatially white noise. Other sources of errors include inaccurate calibration and insufficient SNR for resolving within-beamwidth emitters.

Below, we display the results for the various methods along with the theoretical DOAs. However, one should bear

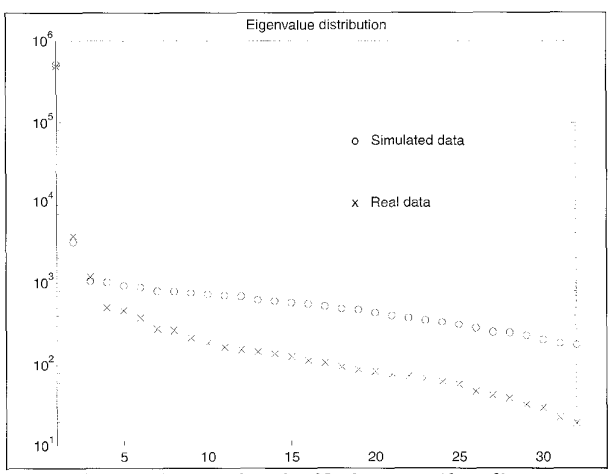

7. Distribution of eigenvalues for 32-element uniform linear array. Simulated and real data.

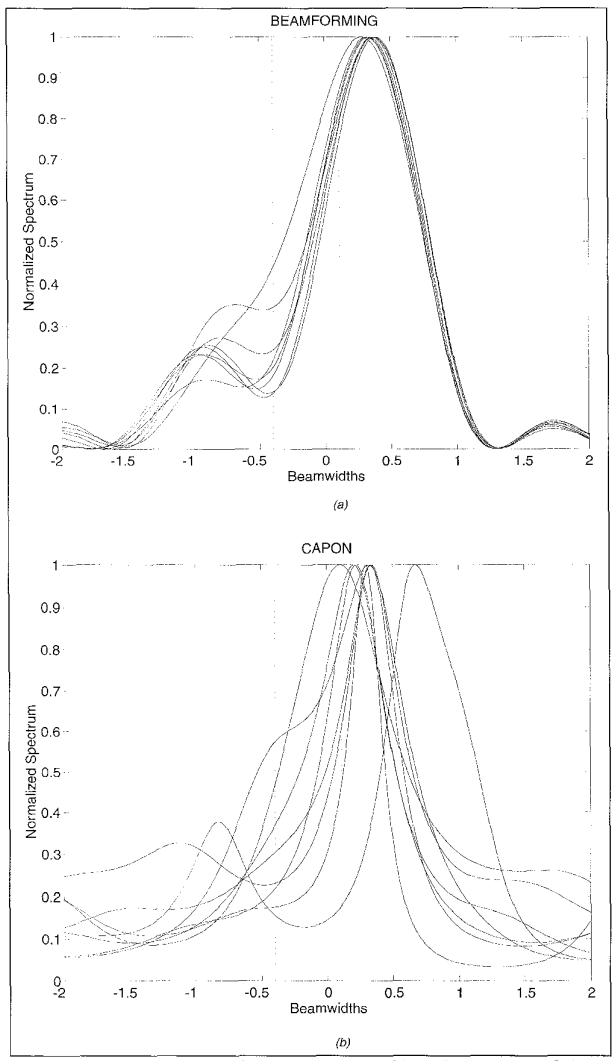

8. Spatial spectra for the beamforming (left) and Capon (right) methods. The results from the 8 batches of the 12.34 GHz data are overlayed. The horizontal axis contains the electrical angle in fractions of the beamwidth. "True" DOAs indicated by vertical dotted lines.

in mind that in a real data experiment, there are actually no true values available for the estimated parameters. The postulated DOAs are calculated from the geometry of the experimental setup, but in practice the multipath component may very well be absent from some of the data sets, or it may impinge from an unexpected direction. We first apply beamforming techniques to the "simplest" case, which is the 12.34 GHz data. The angle separation is here about $\Delta\phi = BW/2$. In Figure 8, the results from applying the traditional beamforming and the Capon methods to the 8 data batches are presented. The "spatial spectra" are all normalized such that the peak value is unity. The "true" DOAs (electrical angles, measured in fractions of the beamwidth) are indicated by vertical dotted lines in the plot. As expected, the Bartlett beamformer cannot quite resolve the sources and neither can Capon's method in this scenario. The high variance of the

latter is due to the short data record (in fact, the sample covariance matrix is not invertible because $N < L$, so a pseudo-inverse was used in Eq. 32).

Next, the spectral-based subspace methods are applied. Since the signal components are expected to be highly correlated, these methods are likely to fail. However, the signals can be "de-correlated" by pre-processing the sample covariance matrix using forward-backward averaging (42). In Figure 9, the results for the MUSIC method with and without FB averaging are shown. It is clear that FB averaging improves the resolution capability and reduces the variance of the estimates in this case. The Min-Norm method was also applied and the resulting normalized "spatial spectra" are depicted in Fig. 10. The Min-Norm method is known to have better resolution properties than MUSIC because of the inherent bias in the radii of the roots [61, 69]. Indeed, the Min-Norm method performs slightly better than MUSIC in this case, and it nearly resolves the sources even without FB averaging.

Finally, we applied parametric methods to the same data sets. The "optimal" methods described earlier all produced virtually identical estimates in all of the available data sets. Therefore, only those of the WSF method are displayed in the plots.

In Fig. 11, we show the WSF estimates along with those of the ESPRIT method with FB averaging. For comparison, we also applied the WSF method to beamspace data. The beamspace dimension was chosen as $R = 8$, and the transformation matrix was designed as follows: First, new "beamspace outputs" were obtained by summing the outputs of sensors 1-25, 2-26, etc. up to 8-32. This corresponds to 8 parallel Bartlett beamformers, all of them steered to the DOA 0° (but with different phases). The SVD of the corresponding 32×8 transformation matrix (which is a Toeplitz matrix with 1/0 entries) was computed, and its left singular vectors were taken as the beamspace transformation matrix $\mathbf{T}$ (cf. (Eq. 96)). The SVD was applied because it is desirable to have orthonormal columns in the transformation matrix, so as not to destroy the spatial color of the noise (if it was white in the first place). The beamspace data were processed using the WSF method similarly to the element-space version. The

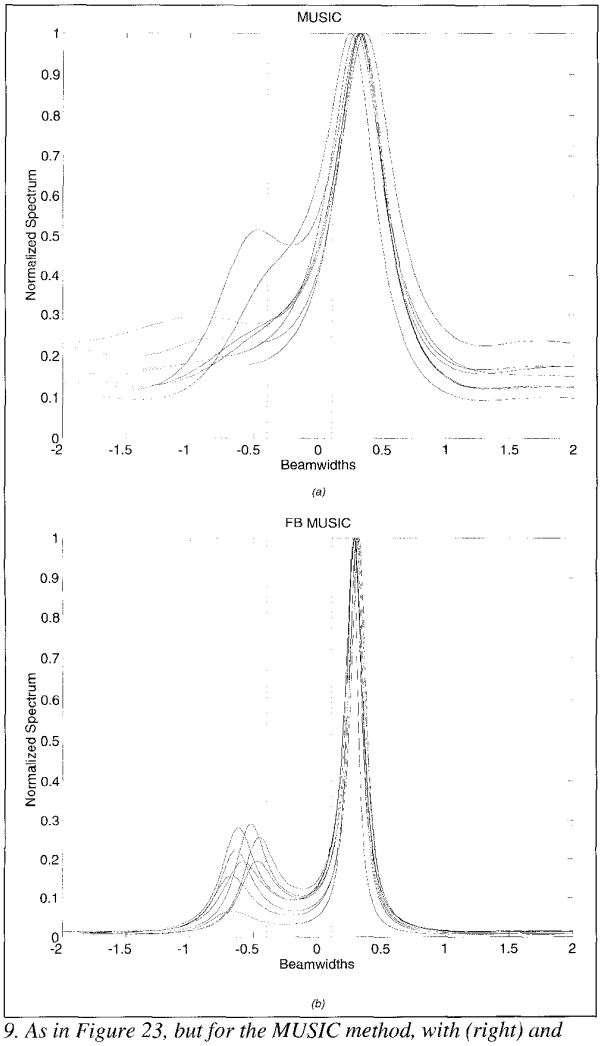

9. As in Figure 23, but for the MUSIC method, with (right) and without (left) forward-backward averaging.

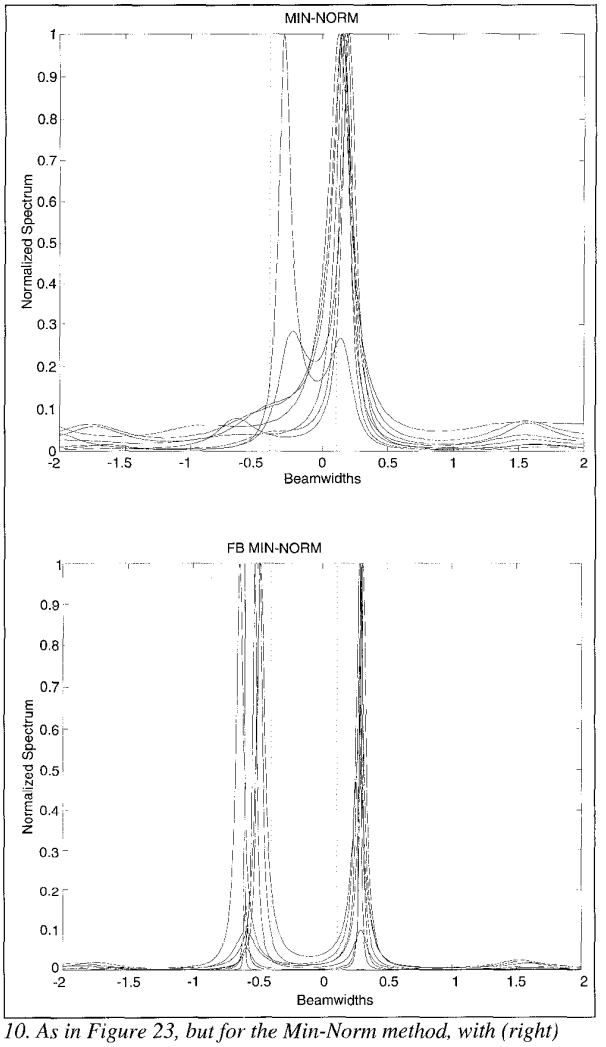

10. As in Figure 23, but for the Min-Norm method, with (right) and without (left) forward-backward averaging.

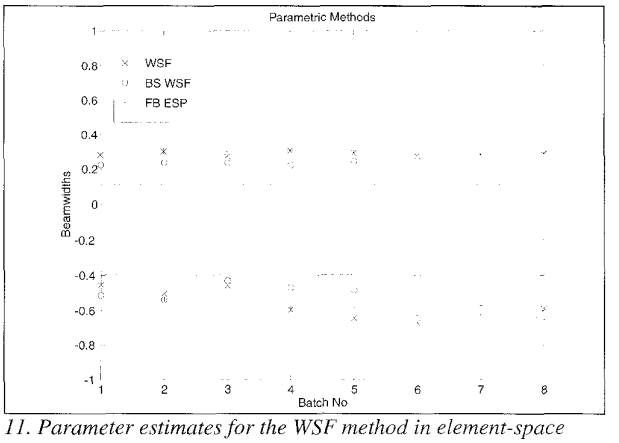

11. Parameter estimates for the WSF method in element-space and beamspace, and for the ESPRIT algorithm with forward-backward averaging. The methods are applied to the 12.34 GHz data.

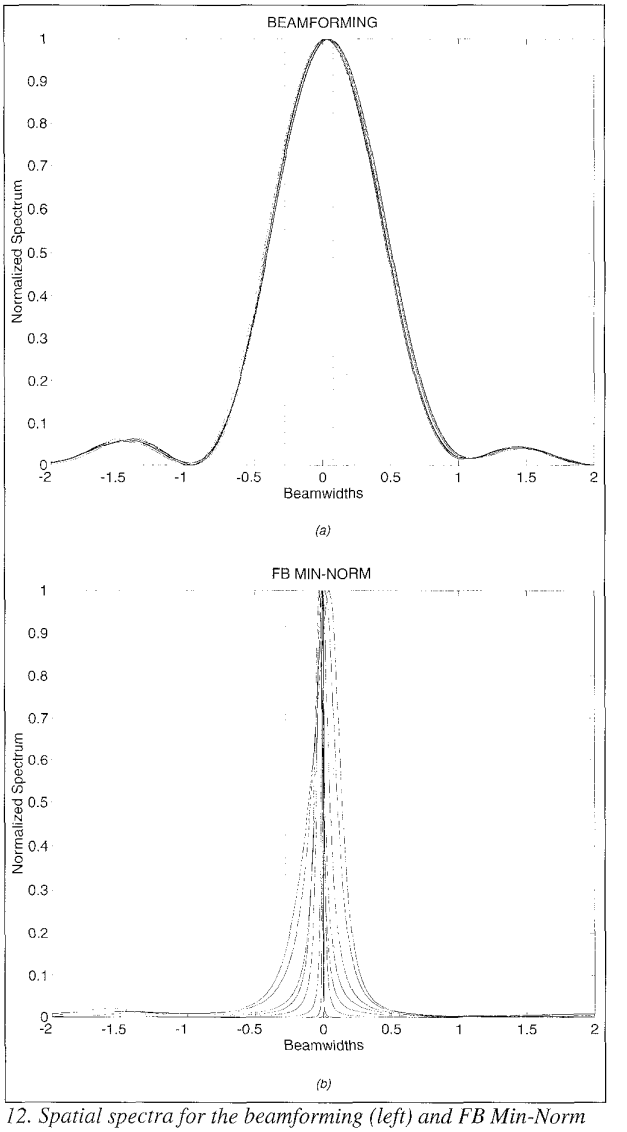

12. Spatial spectra for the beamforming (left) and FB Min-Norm (right) methods applied to the 8.62 GHz data.

results for the parametric methods are shown in Fig. 11. The parametric methods also perform satisfactorily on this data set, and the estimation error is on the order of a 10:th of a beamwidth. This is clearly smaller than for any of the spectral-based methods.

Next, we applied the various algorithms to a more difficult case, namely the 8.62 GHz data. The results for the Bartlett beamformer and the FB Min-Norm method are shown in Fig. 12. It is clear that the spectral-based methods as applied here fail to locate the multipath component. It is possible that other modifications such as spatial smoothing or beamspace processing can improve the situation, but such a test falls beyond the scope of this study.

The estimation results for the parametric methods, applied to the remaining data sets, are shown in Figs. 13 and 14. As seen in the figures, the WSF method performs reasonably well in all data sets except for the one at 9.76 GHz where only one signal is detected, although there is a large bias in the estimate of the multipath component in the 8.62 GHz data. The FB ESPRIT method on the other hand, produces good estimates in half of the batches at 8.62 GHz and fails in most other cases. It is also clear that beamspace processing further improves the parametric methods (not only true for WSF). For the BS WSF method, the estimation errors are less than 20% of the beamwidth with few exceptions. The most likely explanation for the enhanced performance is that beamspace processing reduces the effects of modeling errors. This is made possible by incorporation *a priori* knowledge of the approximate source locations. We also used the DOA estimates to give estimates of the SNR and the signal correlation in the different data sets. The BS WSF estimates at batch 4, were applied to the expressions (59) and (60) to solve for the noise variance and the signal covariance matrix respectively. The results are displayed in Table 3. Note that the signal correlation is defined at the center of the array. Since the aperture is rather large, the correlation phase varies significantly among the sensors. The magnitude of the correlation is close to one in all data sets, indicating that there is indeed a specular multipath. It is a bit curious that the multipath component appears stronger than the direct path in the 8.62

Table 3: Estimated Signal-to-Noise Ratios and Signal Correlation (at the center of the array) for the MARS Data.

Frequency (GHz)	8.62	9.76	9.79	11.32	12.34
SNR direct	9 dB	13 dB	14 dB	10 dB	16 dB
SNR specular	13 dB	10 dB	10 dB	1 dB	10 dB
Correlation	e^{-j123°	e^{-j123°	e^{-j144°	$0.98\, e^{j157^\circ}$	$0.99\, e^{j87^\circ}$

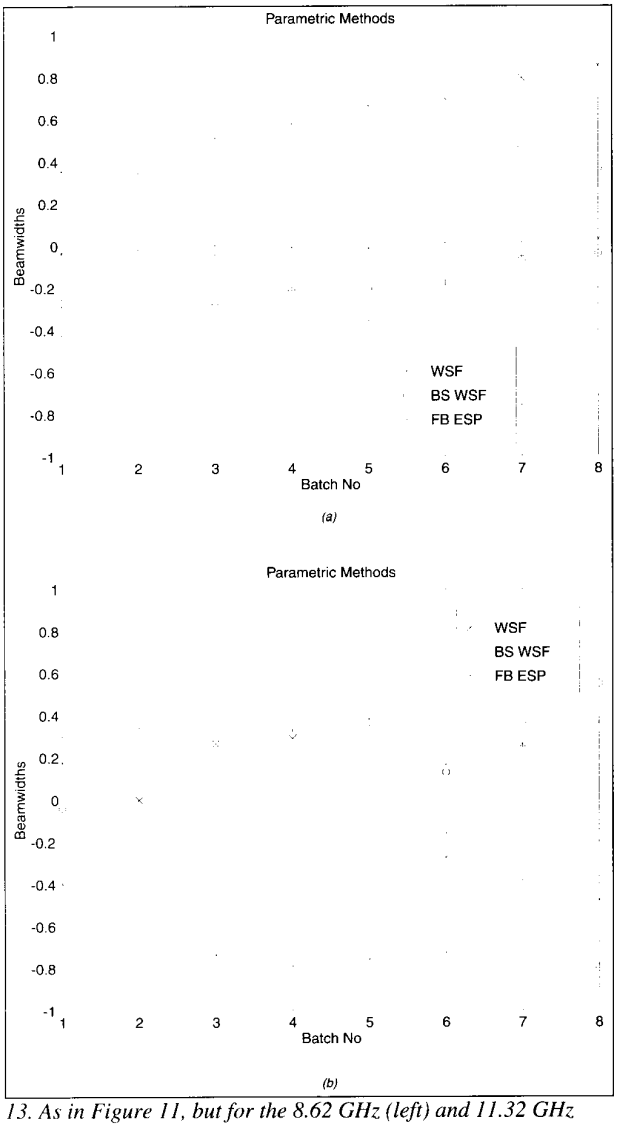

13. As in Figure 11, but for the 8.62 GHz (left) and 11.32 GHz (right) data.

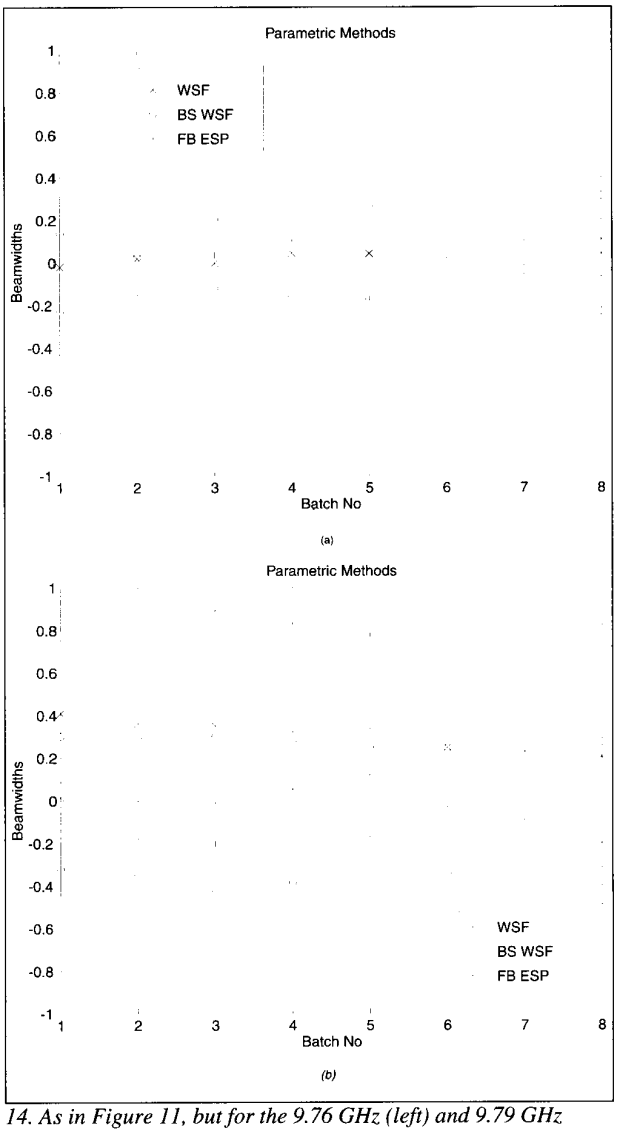

14. As in Figure 11, but for the 9.76 GHz (left) and 9.79 GHz (right) data.

GHz data. This is obviously intriguing, and perhaps it gives an indication of the expected accuracy of the SNR estimates. Another possibility is that more than one reflected component constructively interfered to give one diffuse specular component.

A Manufacturing Example

In the steady march towards a fully automated factory environment, different techniques are constantly being explored for various stages of a production line. Applications of sensor array processing to quality assurance and fault detection have recently been reported [2, 53]. A linear array of photosensors placed along one side of a target is shown in Figure 15 and data is accordingly collected. Assuming that the image of interest is quantized to 1 bit (i.e. 1/0 pixels), a simplified data model follows by assigning data z_l to a sensor in row l as,

$$z_l = \sum_{k=1}^{K} e^{-jx_{kl}}, \; l = 1,\ldots,L$$

where $x_{1l},\ldots,x_{Kl}$ represent the 1-pixels in the l: th row. If the image contains a single straight line as in Fig. 15, there will be only one non-zero pixel in each row, and a little geometry shows that

$$z_l = e^{-jx_0} e^{j(l-1)\tan\theta},$$

where x_0 is the offset and θ is the orientation of the line. The vector of "sensor outputs" is modeled as a complex sinusoid with the row number being the analog of sensor index in our formulation previously. The line offset and orientation can be easily computed from the amplitude and frequency of the sinusoid. The model is straightforwardly extended to the multiple-lines case in gray-scale images, and objects other than lines in the image will appear as noise in the data model. Given the sum-of-sinusoids model, Aghajan and Kailath [2]

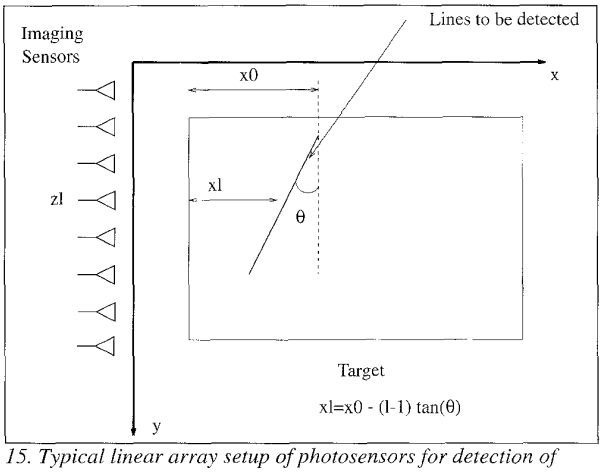

15. Typical linear array setup of photosensors for detection of lines (defects) in a manufacturing environment, by merely using

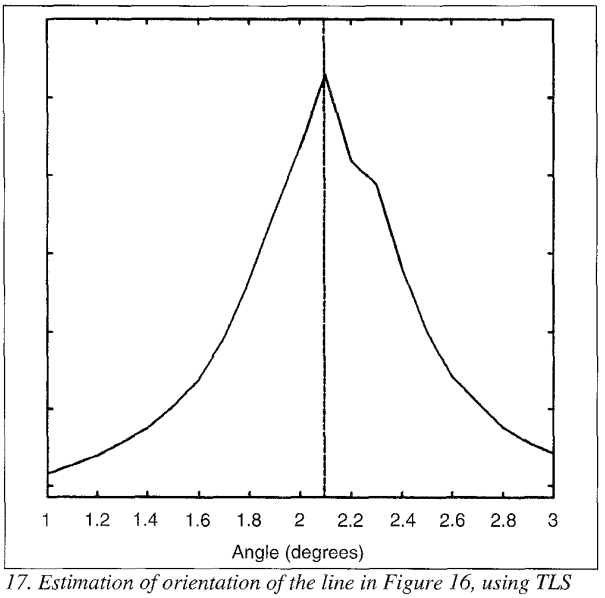

17. Estimation of orientation of the line in Figure 16, using TLS ESPRIT (vertical line) and the Hough transform. The peak magnitude of Hough Transform yields a similar orientation as TLS ESPRIT

suggested to apply the computationally efficient TLS ESPRIT algorithm to spatially smoothed data to obtain estimates of the frequencies and amplitudes.

For illustration purposes, an image of a semiconductor wafer is shown in Fig. 16. A line/scratch is manifested as a bright line of pixels. Anomalous pixels (This may be a defect in the wafer or an inscription put in for orientation.) are on a line typically of brighter intensity and are to be detected and localized. The results of estimating the line orientation by a subspace-based detector (dashed) and by the more classical Hough transform (solid) are displayed in Fig. 17. Figure 18 shows the corresponding result for the line offset estimates. Though the two methods relatively perform equally well, the computational and storage efficiency are not an asset for the Hough transform [2]. In light of the comparison of a subspace-based technique to the more classical approach from

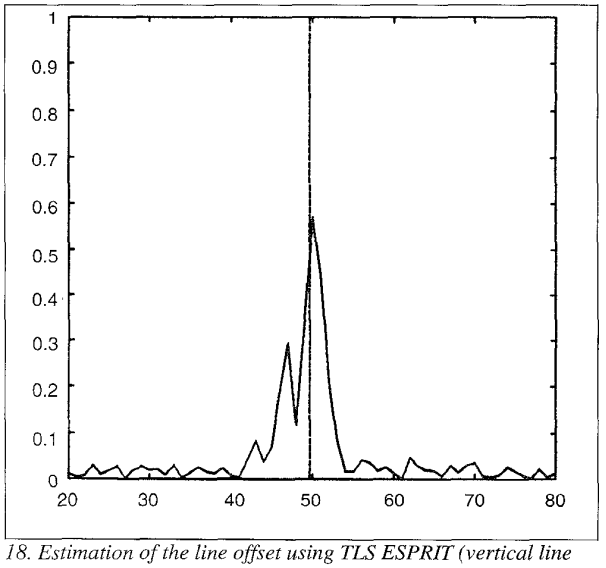

18. Estimation of the line offset using TLS ESPRIT (vertical line and Hough Transform

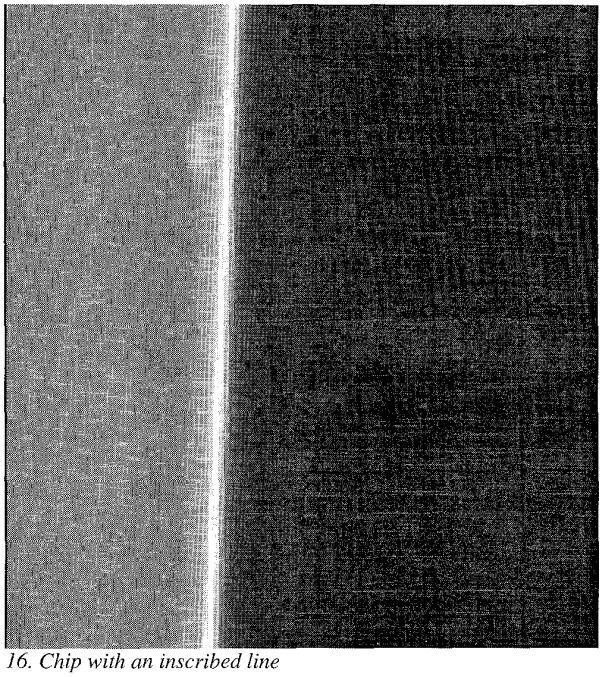

16. Chip with an inscribed line

tomography, namely the Hough transform, shown in these figures, there is reason to believe that sensor array processing solutions need no longer be limited to the framework they were developed in (i.e. signal processing in Radar, Sonar etc.) and potentially offer a wealth of efficient and highly performing algorithms.

Conclusions

The depth acquired from the theoretical research in sensor array processing reviewed in this paper has played a key role in helping identify areas of applications. New real-world

problems which are solvable using array signal processing techniques are regularly introduced, and it is expected that their importance will only grow as automatization becomes more widespread in industry, and as faster and cheaper digital processing systems become available. This manuscript is not meant to be exhaustive, but rather to serve as a broad review of the area, and more importantly as a guide for a first time exposure to an interested reader. The focus is on algorithms, whereas deeper analyses and other more specialized research topics are only briefly touched upon.

In concluding, the recent advances of the field, we think it is safe to say that the spectral-based subspace methods and, in particular, the more advanced parametric methods have clear performance improvements to offer as compared to beamforming methods. Resolution of closely spaced sources (within fractions of a beamwidth) have been demonstrated and documented in several experimental studies. However, high performance is not for free. The requirements on sensor and receiver calibration, mutual coupling, phase stability, dynamic range, etc. become increasingly more rigorous with higher performance specifications. Thus, in some applications the cost for achieving within-beamwidth resolution may still be prohibitive.

The quest for algorithms that perform well under ideal conditions and the understanding of their properties has in some sense slowed down in light of the advances over the past years. However, the remaining work is no less challenging, namely to adapt the theoretical methods to fit the particular demands in specific applications. For example, real-time requirements may place high demands on algorithmic simplicity, and special array and signal structures present in certain scenarios must be exploited. The future work, also in academic research, will be much focused on bridging the gap that still exists between theoretical methods and real-world applications.

Acknowledgments

The authors are grateful to Professor Simon Haykin of McMaster University, for providing the data used in the Measured Data Experiment section and to H. Aghajan of Stanford Univesity for providing figures in the Manufacturing Example section. The authors are also grateful to the reviewers who, through numerous comments, made this paper more readable. One of us is also grateful to Prof. A.S. Willsky of MIT for his constant encouragement and never ending enthusiasm.

Hamid Krim is with the Stocastic Systems Group, LIDS, Massachusetts Institute of Technology, Cambridge, MA 02139.

Mats Viberg is with the Department of Applied Electronics, Chalmers University of Technology, Gothenburg, Sweden.

References

1. B.G. Agee, A.V. Schell, and W.A. Gardner. "Spectral Self-Coherence Restoral: A New Approach to Blind Adaptive Signal Extraction Using Antenna Arrays." *Proc. IEEE*, 78:753-767, Apr. 1990.

2. H.K. Aghajan and T. Kailath. "Sensor Array Processing Techniques for Super Resolution Multi-Line-Fitting and Straight Edge Detection." *IEEE Trans. on Image Proc.*, 2(4), Oct. 1993.

3. S. Anderson, M. Millnert, M. Viberg, and B. Wahlberg. "An Adaptive Array for Mobile Communication Systems." *Trans. on veh. Tec.*, 40, 1991.

4. T.W. Anderson. *An Introduction to Multivariate Statistical Analysis, 2nd edition.* John Wiley& Sons, New York, 1984.

5. S. Andersson. "Optimal Dimension Reduction for Sensor Array Signal Processing." *Signal Processing*, 30(2), Jan. 1993.

6. S.P. Applebaum. "Adaptive Arrays." *IEEE Trans. Antennas and Propagation*, 24(9):585-598, Sept. 1976.

7. Articles. "Spectra From Various Techniques." *IEEE Proceedings*, 69(11), 1981. Special Issue.

8. Articles. "Time Delay Estimation." *IEEE Trans. on Acoustics, Speech and Signal Proc.*, ASSP-29(3), June 1981. Special Issue.

9. Articles. Spectral Estimation. *IEEE Proceedings*, 70(9), 1982. Special Issue.

10. A.B. Baggeroer, W.A. Kuperman, and H. Schmidt. "Matched field processing: Source localization in correlated noise as an optimum parameter estimation problem." *J. Acoust. Soc. Am.*, 83(2):571-587, February 1988.

11. A.J. Barabell. "Improving the Resolution Performance of Eigenstructure-Based Direction-Finding Algorithms." In *Proc. ICASSP 83*, pages 336-339, Boston, MA, 1983.

12. M.S. Bartlett. "Smoothing Periodograms from Time Series with Continuous Spectra." *Nature*, 161:686-687, 1948.

13. G. Bienvenu and L. Kopp. "Adaptivity to Background Noise Spatial Coherence for High Resolution Passive Methods." In *Int. Conf. on Acoust., Speech and Signal Processing*, pages 307-310, 1980.

14. G. Bienvenu and L. Kopp. "Méthodes Haute Resolution Apres Formation de Voies." In *Conference du GRETSI*, volume 1, pages 325-330, Nice, France, May 1985.

15. J.F. Böhme. "Estimation of Source Parameters by Maximum Likelihood and Nonlinear Regression." In *Proc. ICASSP 84*, pages 7.3.1-7.3.4, 1984.

16. J.F. Böhme. "Estimation of Spectral Parameters of Correlated Signals in Wavefields." *Signal Processing*, 10:329-337, 1986.

17. J.F. Böhme. "Statistical Array Signal Processing of Measured Sonar and Seismic Data." In *Proc. SPIE 2563 Advanced Signal Processing Algorithms*, San Diego, CA, 1995.

18. J.F. Böhme and D. Kraus. "On Least Squares Methods for Direction of Arrival Estimation in the Presence of Unknown Noise Fields." In *Proc. ICASSP 88*, pages 2833-2836, New York, N.Y., 1988.

19. Y. Bresler and A. Macovski. "Exact Maximum Likelihood Parameter Estimation of Superimposed Exponential Signals in Noise." *IEEE Trans. ASSP*, ASSP-34:1081-1089, Oct. 1986.

20. Y. Bresler and A. Macovski. "On the Number of Signals Resolvable by a Uniform Linear Array." *IEEE Trans. ASSP*, ASSP-34:1361-1375, Oct. 1986.

21. K. Buckley and X.-L. Xu. "Spatial-Spectrum Estimation in a Location Sector." *IEEE Trans. ASSP*, 38:1842-1852, Nov. 1990.

22. K.M. Buckley and L.J. Griffiths. "An Adaptive Generalized Sidelobe Canceller with Derivative Constraints." *IEEE Trans. on Antennas and Propagation*, AP-34(3):3111-319, 1986 1986.

23. J. Burg. "Maximum Entropy Spectral Analysis." *In 37th Meeting Society Exploration Geophysicists*, 1967.

24. J.A. Cadzow. "Multiple Source Location-The Signal Subspace Approach." *IEEE Trans. ASSP*, ASSP-38:1110-1125, July 1990.

25. J. Capon. "High-Resolution Frequency-Wavenumber Spectrum Analysis." *Proc. IEEE*, 57(8):2408-1418, Aug. 1969.

26. Chen and Y.-S. Lin. "DOA estimation by fourth-order cumulants in unknown noise environments." In *Proc. IEEE ICASSP*, volume 4, pages 296-299, Minneapolis, MN, Apr. 1993.

27. H. Clergeot, S. Tressens, and A. Ouamri. "Performance of High Resolution Frequencies Estimation Methods Compared to the Cramér-Rao Bounds." *IEEE Trans. ASSP*, 37(11):1703-1720, November 1989.

28. P. Comon and G.H. Golub. "Tracking a Few Extreme Singular Values and Vectors in Signal Processing." *Proceedings of the IEEE*, 78:1327-1343, Aug. 1990.

29. J.H. Cozzens and M.J. Sousa. "Source Enumeration in a Correlated Signal Environment." *IEEE Trans. on Acoust., Speech and Signal Proc.*, 42(2):304-317, Feb. 1994.

30. R. DeGroat. "Noniterative Subspace Tracking." *IEEE Trans on SP*, 40(3):571-577, 1992.

31. A. Di. "Multiple Source Location-a Matrix Decomposition Approach." *IEEE Trans. on Acoustics, Speech and Signal Processing*, ASSP-33:1086-1091, Oct. 1985.

32. A. Drosopoulos and S. Haykin. "Adaptive Radar Parameter Estimation with Thomson's Multiple Window Method." In S. Haykin, editor, *Adaptive Radar Detection and Estimation*. John Wiley, New York, 1992.

33. J.E. Evans, J.R. Johnson, and D.F. Sun. "Application of Advanced Signal Processing Techniques to Angle of Arrival Estimation in ATC Navigation and Surveillance Systems." Technical report, MIT Lincoln Laboratory, June 1982.

34. A. Farina. *Antenna-Based Signal Processing Techniques for Radar Systems*. Artech House, Norwood, MA, 1992.

35. D.R. Farrier and L.R. Prosper. "A Signal Subspace Beamformer." In *Proc. ICASSP 90*, pages 2815-2818, Albuquerque, NM, 1990.

36. A.J. Fenn, C.J. Diederich, and P.R. Stauffer. "An Adaptive-Focusing Algorithm for a Microwave Planar Phased-Array Hyperthermia System." *The Lincoln Laboratory Journal*, 6(2):269-288, 1993.

37. A.J. Fenn and G.A. King. "Adaptive Nulling in the Hyperthermia Treatment of Cancer." *The Lincoln Laboratory Journal*, 5(2):223-240, 1992.

38. A.J. Fenn and G.A. King. "Adaptive radio-frequency hyperthermia-phased array system for improved cancer therapy: phantom target measurements." *International Journal of Hyperthermia*, 10(2):189-208, March-April 1994.

39. E.R. Ferrara and T.M. Parks. "Direction Finding with an Array of Sensors Having Diverse Polarizations." *IEEE Trans. on AP*, 31(2):231-236, Mar. 1983.

40. P. Forster. *Méthodes De Traitement d'Antenne Aprés Filtrage Spatial*. Ph.D. thesis, Université de Rennes, France, 1988.

41. P. Forster and G. Vezzosi. "Application of Spheroidal Sequences to Array Processing." In *Proc. ICASSP 87*, 2268-2271, Dallas, TX, 1987.

42. B. Friedlander. "Sensitivity Analysis of the Maximum Likelihood Direction-Finding Algorithm." *IEEE Trans. AES*, AES-26(6):953-968, Nov. 1990.

43. B. Friedlander and A. Weiss. "Direction Finding Using Spatial Smoothing with Interpolated Arrays." *IEEE Trans. AES*, 28:574-587, Apr. 1992.

44. O.L. Frost. "An Algorithm for Linearly Constrained Adaptive Array Processing." *Proc. of the IEEE*, 60(8):926-935, August 1972.

45. W.F. Gabriel. "Spectral Analysis and Adaptive Array Superresolution Techniques." *Proceedings of the IEEE*, 68(6):654-666, June 1980.

46. G.H. Golub and C.F. VanLoan. "An Analysis of the Total Least Squares Problem." *SIAM J. Num. Anal.*, 17:883-893, 1980.

47. G.H. Golub and C.F. VanLoan. *Matrix Computations*. Johns Hopkins University Press, Baltimore, MD., second edition, 1989.

48. R.P. Gooch and J. Lundel. "The CM Array: An Adaptive Beamformer for Constant Modulus Signals." In *Proc. ICASSP 86*, pages 2523-2526, Tokyo, Japan, 1986.

49. N. Härle and J.F. Böhme. "Detection of Knocking for Spark Ignition Engines Based on Structural Vibrations." In *Int. Conf. on Acoust., Speech and Signal Processing*, pages 1744-1747, 1987.

50. S. Haykin, editor. *Array Signal Processing*. Prentice-Hall, Englewood Cliffs, NJ, 1985.

51. S. Haykin. "Radar Array Processing for Angle of Arrival Estimation." In S. Haykin, editor, *Array Signal Processing*. Prentice-Hall, Englewood Cliffs, NJ, 1985.

52. S. Haykin, J. Litva, and T.J. Shepherd (eds). *Radar Array Processing*. Springer-Verlag, Berlin, 1993.

53. L.P. Heck. "Signal Processing Research in Automatic Tool Wear Monitoring." In *ICASSP proceedings*, volume I, pages 55-58, Minneapolis, Min., 1993.

54. B. Hochwald and A. Nehorai. "Concentrated Cramér-Rao Bound Expressions." *IEEE Trans. on IT*, 40(2):363-371, Mar. 1994.

55. Harold Hotelling. "Analysis of a Complex of Statistical Variables into Principal Components." *J. Educ. Psych.*, 24:417-441,498-520, 1933.

56. H. Hung and M. Kaveh. "Focussing Matrices for Coherent Signal-Subspace Processing." *IEEE Trans. ASSP*, ASSP-36:1272-1281, Aug. 1988.

57. A.G. Jaffer. "Maximum Likelihood Direction Finding of Stochastic Sources: A Separable Solution." In *Proc. ICASSP 88*, volume 5, pages 2893-2896, New York, New York, April 1988.

58. Don H. Johnson and Dan E. Dudgeon. *Array Signal Processing -Concepts and Techniques*. Prentice-Hall, Englewood Cliffs, NJ, 1993.

59.. C. Jordan and K. G. Balman. *Electromagnetic Waves and Radiating Systems*. Prentice-Hall, New Jersey, second edition, 1968.

60. I. Karasalo. "Estimating the Covariance Matrix by Signal Subspace Averaging." *IEEE Trans. ASSP*, ASSP-34(1):8-12, February 1986.

61. M. Kaveh and A.J. Barabell. "The Statistical Performance of the MUSIC and the Minimum-Norm Algorithms in Resolving Plane Waves in Noise." *IEEE Trans. ASSP*, ASSP-34:331-341, April 1986.

62. M. Kaveh and A. Bassias. "Threshold Extension Based on a New Paradigm for MUSIC-type Estimation." In *Proc. ICASSP 90*, pages 2535-2538, Albuquerque, NM, April 1990.

63. S. Kay. *Fundamentals of Statistical Signal Processing: Estimation Theory*. Prentice-Hall International Editions, Englewood Cliffs, NJ, 1993.

64. S.M. Kay and V. Nagesha. "Maximum Likelihood Estimation of Signals in Autoregressive Noise." *IEEE Trans on SP*, 42:88-101, Jan. 1994.

65. T. Koopmans. *Linear Regression Analysis of Economic Time Series*. Haarlem, De Erven F. Bohn N.V., 1937.

66. D. Kraus and J.F. Böhme. "Maximum Likelihood Location Estimation of Wideband Sources Using the EM Algorithm." In *Adapt. Syst. in Contr. and Sig. Proc. 1992. Selected Papers from the 4th IFAC Symposium*, pages 487-491, Grenoble, France, 1993.

67. H. Krim and J.H. Cozzens. *Detection and Parameter Estimation of Correlated Signals in Noise*. Ph.D. thesis, Northeastern. Univ., June 1991.

68. H. Krim. "A Data-Based Enumeration of Fully Correlated Signals." *IEEE Trans. Acoust., Speech, Signal Processing*, July 1994.

69. H. Krim, P. Forster, and J.G. Proakis. "Operator Approach to Performance Analysis of Root-MUSIC and Root Min-Norm." *IEEE Trans. Acoust., Speech, Signal Processing*, 40, July 1992.

70. H. Krim and J.G. Proakis. "Smoothed Eigenspace-Based Paramerter Estimation." *Automatica, Special Issue on Statistical Signal Processing and Control*, Jan. 1994.

71. J. Krolik. "Focused Wideband Array Processing for Spatial Spectral Estimation." In S. Haykin, editor, *Advances in Spectrum Analysis and Array Processing*, volume 2. Prentice-Hall, Englewood Cliffs, NJ, 1991.

72. R. Kumaresan and D.W. Tufts. "Estimating the Angles of Arrival of Multiple Plane Waves." *IEEE Trans. on Aeros. and Elect. Sys.*, AES-19(1), January 1983.

73. S.Y. Kung. "A New Identification and Model Reduction Algorithm via Singular Value Decomposition." In *Proc. 12th Asilomar Conf. on Circuits, Systems and Computers*, pages 705-714, Pacific Grove, CA, November 1978.

74. R.T. Lacoss. "Data Adaptive Spectral Analysis Methods." *Geophysics*, 36:661-675, 71.

75. F. Li, J. Vaccaro, and D. W. Tufts. "Min-Norm Linear Prediction For Arbitrary Sensor Arrays." In *Int. Conf. on Acoust., Speech and Signal Processing*, pages 2613-2616, 1989.

76. F. Li and R. Vaccaro. "Sensitivity Analysis of DOA Estimation Algorithms to Sensor Errors." *IEEE Trans. AES*, AES-28(3):708-717, July 1992.

77. F. Li and R.J. Vaccaro. "Performance Degradation of DOA Estimators Due to Unknown Noise Fields." *IEEE Trans. SP*, SP-40(3):686-689, March 1992.

78. J. Li and P. Stoica. "Efficient Parameter Estimation of Partially Polarized Electromagnetic waves." *IEEE Trans. on SP*, 42(11):3114-3125, Nov. 1994.

79. W.S. Liggett. *Passive Sonar: Fitting Models to Multiple Time Series*, volume Signal Processing, pages 327-345. Academic Press, New York, J.W.R. Griffiths and P.L. Stocklin and C. Vam Schoonefeld edition, 1973.

80. H. Liu, G. Xu, and L. Tong. "A Deterministic Approach to Blind Equalization." In *Proc. of Asilomar*, pages 751-755, Monterey, Nov. 1993.

81. V.H. MacDonald and P.M. Schultheiss. "Optimum Passive Bearing Estimation in a Spatially Incoherent Noise Environment." *J. Acoust. Soc. Am.*, 46(1):37-43, 1969.

82. C.P. Mathews and M. D. Zoltowski. "Eigenstructure Techniques for 2-D Angle Estimation with Uniform Circular Arrays." *IEEE Trans. on SP*, 42:2395-2407, Sept. 1994.

83. P. Milanfar. *Geometric Estimation and Reconstruction from Tomographic Data*. PhD thesis, MIT, Cambridge, MA, 1993.

84. P. Milanfar, G.C. Verghese, W.C. Karl, and A.S. Willsky. "Reconstructing Polygons from Moments with Connections to Array Processing." *IEEE Trans. on Signal Proc.*, To Appear.

85. J.S. Mosher, R.M. Leahy, and P.S. Kewis. "Biomagnetic Localization from Transient Quasi-Static Events." In *Proc. ICASSP 93*, volume 1, pages 91-94, Minneapolis, MN, 1993.

86. A. Nehorai and E. Paldi. "Vector-sensor Array processing for Electromagnetic Source Localization." *IEEE Trans. on SP*, 42(2):376-398, Feb. 1994.

87. A. Nehorai, B. Porat, and E. Paldi. "Detection and Localization of Vapor-Emitting Sources." *IEEE Trans. on SP*, 43:243-253, Jan. 1995.

88. B. Ottersten and T. Kailath. "Direction-of-Arrival Estimation for Wide-Band Signals Using the ESPRIT Algorithm." *IEEE Trans. ASSP*, ASSP-38(2):317-327, Feb. 1990.

89. B. Ottersten, M. Viberg, and T. Kailath. "Analysis of Subspace Fitting and ML Techniques for Parameter Estimation from Sensor Array Data." *IEEE Trans. on SP*, SP-40:590-600, March 1992.

90. B. Ottersten, M. Viberg, P. Stoica, and A. Nehorai. "Exact and large sample ML techniques for parameter estimation and detection in array processing." In Haykin, Litva, and Shepherd, editors, *Radar Array Processing*, pages 99-151. Springer-Verlag, Berlin, 1993.

91. N.L. Owsley. *Sonar Array Processing*, chapter 3, pages 115-184. Haykin, Editor. Prentice Hall, Englewood Cliffs, New Jersey, 1985.

92. A. Paulraj and T. Kailath. "Eigenstructure Methods for Direction-of-Arrival Estimation in the Presence of Unknown Noise Fields." *IEEE Trans. on ASSP*, ASSP-33:806-811, Aug. 1985.

93. A. Paulraj, R. Roy, and T. Kailath. "A Subspace Rotation Approach to Signal Parameter Estimation." *Proceedings of the IEEE*, pages 1044-1045, July 1986.

94. V.F. Pisarenko. "The Retrieval of Harmonics from a Covariance FSunction." *Geophys.* J. Roy. Astron. Soc., 33:347-366, 1973.

95. B. Porat and B. Friedlander. "Direction Finding Algorithms Based on High-Order Statistics." *IEEE Trans. SP*, SP-39:2016-2024, Sept. 1991.

96. J.G. Proakis and D.G. Manolakis. *Digital Signal Processing, second edition*. Macmillan, New York, 1992.

97. B.D. Rao and K.V.S. Hari. "Performance Analysis of ESPRIT and TAM in Determining the Direction of Arrival of Plane Waves in Noise." *IEEE Trans. ASSP*, ASSP-37(12):1990-1995, Dec. 1989.

98. B.D. Rao and K.V.S. Hari. "Performance Analysis of Root-MUSIC." *IEEE Trans. Acoust., Speech, Signal Processing*, 37(12):1939-1949, December 1989.

99. S.S. Reddi. "Multiple Source Location - A Digital Approach." *IEEE Trans. AES*, 15:95-105, Jan. 1979.

100. Y. Rockah and P. M. Schultheiss. "Array Shape Calibration Using Sources in Unknown Locations - Part I: Far-field sources." *IEEE Trans. on ASSP*, 35:286-299, March 1987.

101. R. Roy and T. Kailath. "ESPRIT - Estimation of Signal Parameters via Rotational Invariance Techniques." *IEEE Trans. on ASSP*, ASSP-37(7):984-995, July 1989.

102. Jr. R.T. Compton. *Adaptive Antennas*. Prentice Hall, Englewood Cliffs, NJ, 1988.

103. S. Sakagami, S. Aoyama, K. Kuboi, S. Shirota, and A. Akeyama. "Vehicle Position Estimates by Multibeam Antennas in Multipath Environments." *IEEE Trans. on Vehicular Tech.*, 41(1):63-68, Feb. 1992.

104. S.V. Schell and W.A. Gardner. "Blind adaptive spatiotemporal filtering for wide-band cyclostationary signals." *IEEE Trans. SP*, 41:1961-1964, May 1993.

105. R.O. Schmidt. *A Signal Subspace Approach to Multiple Emitter Location and Spectral Estimation*. Ph.D. thesis, Stanford Univ., Stanford, CA, Nov. 1981.

106. F.C. Schweppe. "Sensor Array Data Processing for Multiple Signal Sources." *IEEE Trans. on IT*, IT-14:294-305, 1968.

107. S. Shamsunder and G. Giannakis. "Signal Selective Localization of NonGaussian Cyclostationary Sources." *IEEE Trans. SP*, 42:2860-2864, Oct. 1994.

108. T.J. Shan, M. Wax, and T. Kailath. "On spatial Smoothing for Directions of Arrival Estimation of Coherent Signals." *IEEE Trans. on Acoustics, Speech and Signal Processing*, ASSp-33(4):806-811, April 1985.

109. S. Sivanand, J.-F. Yang, and M. Kaveh. "Focusing Filters for Wide-Band Direction Finding." *IEEE Trans. SP*, 39:437-445, Feb. 1991.

110. D.T.M. Slock. "Blind Fractionally-Spaced Equalization, Perfect-Reconstruction Filter Banks and Multichannel Linear Prediction." In *Proc. ICASSP 94*, volume 4, pages 585-588, Adelaide, Australia, April 1994.

111. K. Steiglitz and L. McBride. "A Technique for Identification of Linear Systems." *IEEE Trans. Autom. Contr.*, AC-10:461-464, Oct. 1965.

112. P. Stoica and A. Nehorai. "MUSIC, Maximum Likelihood and Cramér-Rao Bound." *IEEE Trans. ASSP*, ASSP-37:720-741, May 1989.

113. P. Stoica and A. Nehorai. "MODE, Maximum Likelihood and Cramér-Rao Bound: Conditional and Unconditional Results." In *Proc. ICASSP 90 Conf*, pages 2715-2718, Albuquerque, NM, April 1990.

114. P. Stoica and A. Nehorai. "MUSIC, Maximum Likelihood and Cramér-Rao Bound: Further Results and Comparisons." *IEEE Trans. ASSP*, ASSP-38:2140-2150, December 1990.

115. P. Stoica and A. Nehorai. "Performance Study of Conditional and Unconditional Direction-of-Arrival Estimation." *IEEE Trans. ASSP*, ASSP-38:1783-1795, October 1990.

116. P. Stoica and K. Sharman. "A Novel Eigenanalysis Method for Direction Estimation." *Proc. IEE*, F:19-26, Feb 1990.

117. P. Stoica and K. Sharman. "Maximum Likelihood Methods for Direction-of-Arrival Estimation." *IEEE Trans. ASSP*, ASSP-38:1132-1143, July 1990.

118. P. Stoica and T. Söderström. "Statistical Analysis of MUSIC and Subspace Rotation Estimates of Sinusoidal Frequencies." *IEEE Trans. ASSP*, ASSP-39:1836-1847, Aug. 1991.

119. P. Stoica, M. Viberg, and B. Ottersten. "Instrumental Variable Approach to Array Processing in Spatially Correlated Noise Fields." *IEEE Trans. SP*, SP-42:121-133, Jan. 1994.

120. M. Stojanovic and Z. Zvonar. "Adaptive Spatial/Temporal Multiuser Receivers for Time-Varying Channels with Severe Isi." In *Proc. of Conf. on Signals and Systems*, Princeton, March 1994.

121. E. Ström, S. Parkvall, and B.Ottersten. "Near-far Resistant Propagation Delay Estimators for Asynchronous Direct-sequence Code Division Multiple Access Systems." In C.G. Gunther, editor, *Mobile Communications. Advanced Systems and Components. 1994 International Zürich Seminar on*

Digital Communications Proceedings, pages 251-260, Zürich, Switzerland, March 1994. Springer-Verlag.

122. G. Su and M. Morf. "Modal Decomposition Signal Subspace Algorithms." *IEEE Trans. ASSP*, ASSP-34(3):585-602, June 1986.

123. S.C. Swales, M.A. Beach, and D.J. Edwards. "Multi-Beam Adaptive Base Station Antennas for Cellular Land Mobile Radio Systems." In *Proc. IEEE Veh. Technol. Conf.*, pages 341-348, 1989.

124. A. Swindlehurst and T. Kailath. "Passive direction-of-arrival and Range Estimation for Near-field Sources." In *Proc. 4th ASSP Workshop on Spectral Estimation and Modeling*, pages 123-128, Minneapolis, MN, August 1988.

125. A. Swindlehurst and T. Kailath. "A Performance Analysis of Subspace-Based Methods in the Presence of Model Errors - Part I: The MUSIC Algorithm." *IEEE Trans. SP*, SP-40(7):1758-1774, July 1992.

126. A. Swindlehurst and T. Kailath. "A Performance Analysis of Subspace-Based Methods in the Presence of Model Errors: Part 2 - Multidimensional Algorithms." *IEEE Trans. on SP*, SP-41:2882-2890, Sept. 1993.

127. A.L. Swindlehurst and M. Viberg. "Subspace Fitting with Diversely Polarized Antenna Arrays." *IEEE Trans. on AP*, 41:1687-1694, Dec. 1993.

128. S. Talwar, M. Viberg, and A. Paulraj. "Estimating Multiple Co-Channel Digital Signals Using an Antenna Array." *IEEE SP Letters*, 1:29-31, Feb. 1994.

129. L. Tong, G. Xu, and T. Kailath. "A New Approach to Blind Identification and Equalization of Multipath Channels." *IEEE Trans. on Inf. Theory*, To appear.

130. H. L. Van Trees. *Detection, Estimation and Modulation Theory, part. I.* J. Wiley & Sons Inc., 1968.

131. F. Tuteur and Y. Rockah. "A New Method for Detection and Estimation Using the Eigenstructure of the Covariance Difference." In *Proc. ICASSP 88 Conf*, pages 2811-2814, Tokyo, Japan, 1986.

132. B.D. Van Veen and K.M. Buckley. "Beamforming: A Versatile Approach to Spatial Filtering." *IEEE ASSP Magazine*, pages 4-24, April 1988.

133. B.D. Van Veen and B. Williams. "Dimensionality Reduction in High Resolution Direction of Arrival Estimation." In *Proc. Asilomar Conf. Sig., Syst., Comput.*, Pacific Groove, CA, Oct. 1988.

134. M. Viberg. "On Subspace-Based Methods for the Identification of Linear Time-Invariant Systems." *Automatica*, Dec. 1995.

135. M. Viberg and B. Ottersten. "Sensor Array Processing Based on Subspace Fitting." *IEEE Trans. SP*, SP-39(5):1110-1121, May 1991.

136. M. Viberg, B. Ottersten, and T. Kailath. "Detection and Estimation in Sensor Arrays Using Weighted Subspace Fitting." *IEEE Trans. SP*, SP-39(11):2436-2449, Nov. 1991.

137. M. Viberg and A.L. Swindlehurst. "A Bayesian Approach to Auto-Calibration for Parametric Array Signal Processing." *IEEE Trans. SP*, 42, Dec. 1994.

138. M. Viberg and A.L. Swindlehurst. "Analysis of the Combined Effects of Finite Samples and Model Errors on Array Processing Performance." *IEEE Trans. SP*, 42:3073-3083, Nov. 1994.

139. Mats Viberg. "Sensitivity of Parametric Direction Finding to Colored Noise Fields and Undermodeling." *Signal Processing*, 34(2):207-222, Nov. 1993.

140. H. Wang and M. Kaveh. "Coherent Signal-Subspace Processing for the Detection and Estimation of Angles of Arrival of Multiple Wide-Band Sources." *IEEE Trans. ASSP*, ASSP-33:823-831, Oct. 1985.

141. M. Wax. *Detection and Estimation of Superimposed Signals.* PhD thesis, Stanford Univ., Stanford, CA, March 1985.

142. M. Wax. "Detection and Localization of Multiple Sources in Noise with Unknown Covariance." *IEEE Trans. on ASSP*, ASSP-40(1):245-249, Jan. 1992.

143. M. Wax and T. Kailath. "Detection of Signals by Information Theoretic Criteria." *IEEE Trans. on Acoustics, Speech and Signal Processing*, ASSP-33(2):387-392, February 1985.

144. M. Wax, T.J. Shan, and T. Kailath. "Spatio-Temporal Spectral Analysis by Eigenstructure Methods." *IEEE Trans. ASSP*, ASSP-32, Aug. 1984.

145. M. Wax and I. Ziskind. "On Unique Localization of Multiple Sources by Passive Sensor Arrays." *IEEE Trans. on ASSP*, ASSP-37(7):996-1000, July 1989.

146. A.J. Weiss and B. Friedlander. "Array Shape Calibration Using Sources in Unknown Locations - A Maximum Likelihood Approach." *IEEE Trans. on ASSP*, 37(12):1958-1966, Dec. 1989.

147. A.J. Weiss and B. Friedlander. "Performance Analysis of Diversely Polarized Antenna Arrays." *IEEE Trans. on SP*, 39(7):1589-1603, July 1991.

148. B. Widrow, K.M. Duvall, R.P. Gooch, and W.C. Newman. "Signal Cancellation Phenomena in Adaptive Antennas: Causes and Cures." *IEEE Trans. Antennas and Propagation*, AP-30(5):469-478, July 1982.

149. N. Wiener. *Extrapolation, Interpolation and Smoothing of Stationary Time Series.* MIT Press, Cambridge, MA, 1949.

150. J.H. Winters. "Optimum Combining for Indoor Radio Systems with Multiple Users." *IEEE Trans. Communications*, 35:1222-1230, 1987.

151. K.M. Wong, J.P. Reilly, Q. Wu, and S. Qiao. "Estimation of the Directions of Arrival of Signals in Unknown Correlated Noise, Parts I and II." *IEEE Trans. on SP*, SP-40:2007-2028, Aug. 1992.

152. Q. Wu and K.M. Wong. "UN-MUSIC and UN-CLE: An Application of Generalized Canonical Correlation Analysis to the Estimation of the Directions of Arrival of signals in unknown correlated noise." *IEEE Trans. SP*, 42:2331-2341, Sept. 1994.

153. G. Xu and T. Kailath. "Direction-of-Arrival Estimation via Exploitation of Cyclostationary-a Combination of Temporal and Spatial Processing." *IEEE Trans. SP*, 40(7):1775-1786, July 1992.

154. G. Xu and T. Kailath. "Fast Subspace Decomposition." *IEEE Trans. SP*, 42(3):539-551, March 1994.

155. W. Xu and M. Kaveh. "Design of Signal-subspace Cost Functionals for Parameter Estimation." In *Proc. ICASSP 92*, volume 5, pages 405-408, San Francisco, CA, Mar. 1992.

156. W. Xu, J. Pierre, and M. Kaveh. "Practical Detection with Calibrated Arrays." In *Proc. 6:th SP Workshop on Statistical Signal and Array Processing*, pages 82-85, Victoria, Canada, Oct. 1992.

157. X.-L. Xu and K. Buckley. "Bias Analysis of the MUSIC Location Estimator." *IEEE Trans. SP*, 40(10):2559-2569, Oct. 1992.

158. X.-L. Xu and K. Buckley. "An analysis of beam-space source localization." *IEEE Trans. SP*, 41(1):501-504, Jan. 1993.

159. J.-F. Yang and M. Kaveh. "Adaptive Eigensubspace Algorithms for Direction or Frequency Estimation and Tracking." *IEEE Trans. ASSP*, 36(2):241-251, Feb. 1988.

160. L.C. Zhao, P.R. Krishnaiah, and Z.D. Bai. "On Detection of the Number of Signals in Presence of White Noise." *J. of Multivariate Analysis*, 20:1:1-25, 1986.

161. I. Ziskind and M. Wax. "Maximum Likelihood Localization of Multiple Sources by Alternating Projection." *IEEE Trans. on ASSP*, ASSP-36:1553-1560, Oct. 1988.

162. I. Ziskind and M. Wax. "Maximum Likelihood Localization of Diversely Polarized Sources by Simulated Annealing." *IEEE Trans. on AP*, 38(7):1111-1114, July 1990.

163. M. D. Zoltowski. "Beamspace ml Bearing Estimation for Adaptive Phased Array Radar." In S. Haykin, editor, *Adaptive Radar Detection and Estimation.* John Wiley, New York, 1992.

164. M.D. Zoltowski, G.M. Kautz, and S.D. Silverstein. "Beamspace Root-MUSIC." *IEEE Trans. on SP*, 41:344-364, Jan. 1993.

165. A.M. Zoubir and J.F. Böhme. "Bootstrap Multiple Tests Applied to Sensor Location." *IEEE Trans. on SP*, 43:1386-1396, June 1995.